Journal of King Saud University – Computer and Information Sciences 35 (2023) 101733

HOSTED BY

Contents lists available at ScienceDirect

Journal of King Saud University – Computer and Information Sciences

journal homepage: www.sciencedirect.com

Multimodal medical image fusion towards future research: A review

Sajid Ullah Khan [a], Mir Ahmad Khan [b], Muhammad Azhar [c], Faheem Khan [d,*], Youngmoon Lee [e,*], Muhammad Javed [f]

[a] Department of Information System, Prince Sattam bin Abdulaziz University, AL-Kharj, Saudi Arabia
[b] Department of Computer Science, University of Lakki Marwat, KPK, Pakistan
[c] Department of Information and Communication Engineering, Chosun University, Gwangju, South Korea
[d] Department of Computer Engineering, Gachon University, Seongnam-si 13120, South Korea
[e] Department of Robotics, Hanyang University, Ansan-si 15558, South Korea
[f] Institute of Engineering and Computing Science, University of Science & Technology, Bannu, KPK, Pakistan

ARTICLE INFO

Article history:
Received 21 April 2023
Revised 30 July 2023
Accepted 24 August 2023
Available online 29 August 2023

Keywords:
Medical Image Fusion
Information fusion
Multimodal Imaging
Fusion Strategy
Fusion Methods

ABSTRACT

Medical imaging has been widely used to diagnose various disorders over the past 20 years. Primary challenges in medicine include accurate disease identification and improved therapies. It is challenging for the medical experts to diagnose diseases using a single imaging modality. The fusion of two or more images obtained from different imaging modalities is known as multi modal image fusion (MMIF).The fused image contains complementary information for all the input images. The main objective of MMIF is to obtain complementary information (structural and spectral) from input images to improve the quality and clear assessment of medical related problems. The aim of fusion process is not only to reduced the amount of data but construct image having more useful and complementary information which are understandable for human and computer. This review provides a detailed overview of: (i) medical imaging modalities, (ii) multimodal medical image databases, (iii) MMIF steps/rules, (iv) MMIF methods, (v) modalities integration, (vi) performance evaluation and empirical results, (vii) current modalities strengths and limitations, and (viii) future directions. This review is expected to be useful in establishing a solid foundation for the development of more valuable medical image fusion methods for clinical diagnosis. This review presented the detailed studies on the multimodal databases, research trends in imaging modality grouping, and fusion steps which are the critical areas in MMIF. Furthermore, current challenges and future directions are thoroughly discussed.

Contents

* Corresponding authors.
E-mail addresses: faheem@gachon.ac.kr (F. Khan), youngmoonlee@hanyang.ac.kr (Y. Lee).

https://doi.org/10.1016/j.jksuci.2023.101733
1319-1578/

1. Introduction

Medical images acquired using different modalities are widely used in medical applications for clinical diagnosis. However, single-mode images generally fail to provide functional and anatomical information. Therefore, the image fusion process combines the complementary information from various imaging modalities that are reliable for clinical purposes. Imaging modalities, such as the magnetic resonance imaging (MRI), computed tomography (CT), positron emission tomography (PET), X-rays, ultrasound (US), and photon emission computed tomography (SPECT) are used for clinical diagnosis and provide information on soft tissues, blood flow, lesion location, and level. Different imaging modalities provide different information on the same organs of the body. Multimodal Medical Image Fusion (MMIF) is crucial in disease diagnosis because it provides functional and structural information about the same organs in the body (Rajalingam and Priya, 2018). The fused image should fulfill the following conditions: (a) it should retain the complementary/detail information of the input images, (b) it should not have artifacts, such as scratches or dots, and (c) it should not have noise and registration issues (James and Dasarathy, 2014). Various studies have indicated the importance of MMIF research. Fig. 1 illustrates the annual publication results of the MMIF, which were obtained from the Web of Science (WoS), a platform that provides access to numerous databases across multiple academic fields.

Various surveys and review articles have summarized the MMIF techniques and classifications (Faragallah et al., 2020; Kaur et al., 2021). Numerous MMIF issues are covered in (Faragallah et al., 2020; Kaur et al., 2021; Huang et al., 2020), wherein an overview of the MMIF techniques, modalities, and performance analysis is presented. However, detailed studies on the multimodal databases, research trends in imaging modality grouping, and fusion steps are lacking. Furthermore, current challenges and future directions have not been thoroughly discussed. The MMIF steps, fusion techniques, and image quality metrics are thoroughly described in (Du et al., 2016); however, this study only provides information on multimodal databases and focuses solely on the (AANLIB) Harvard medical dataset. The classification of medical image registration was presented in (El-Gamal et al., 2016); wherein the MMIF and recent disorders based on the fusion efforts are highlighted. The region-based image fusion methods are described in (Meher et al., 2019); however, the images in this review are from a variety of sources, including multimodal medical images, multi focus images, and infrared rays. A detail review was presented in (Bhosale and Patnaik, 2023) about deep machine learning techniques. This study focuses on DL techniques used for Covid-19 detection systems. This review also discusses different modalities with details analysis. However, this study MMIF techniques, modalities grouping and fusion steps are lacking. Table 1 compares this study with a recent state-of-the-art literature review. The specific contributions of this study are as follows:

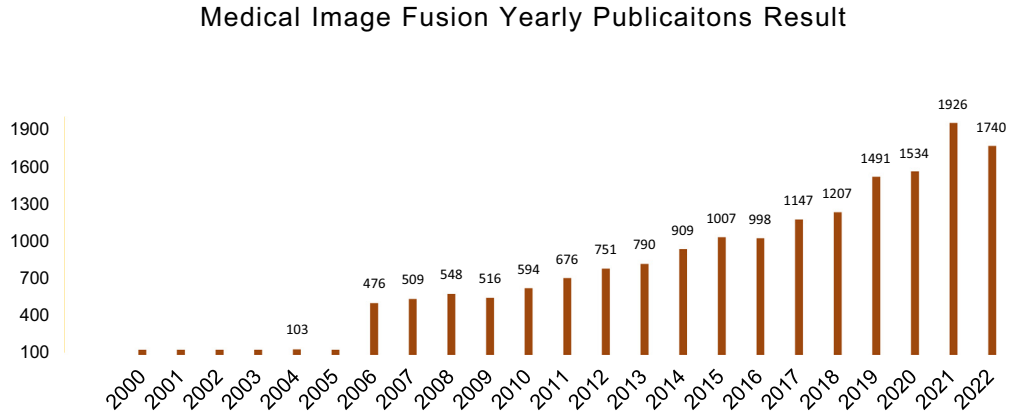

Fig. 1. Annual publication results on MMIF [WoS 2000–2022].

Table 1
Comparison of the recent MMIF reviews of the literature.

Review work (year of publication)	Presented multimodal Imaging modalities sources and methods	Presented MMIF techniques	Quantitative comparison of MMIF techniques	Qualitative comparison of MMIF techniques	Presented publically available databases	Fusion Steps	Ways of Modalities Combination for Image Fusion	Presented performance analysis of MMIF techniques
Rajalingam, B (Rajalingam and Priya, 2018) 2018	√	√	x	x	x	x	x	x
Dolly, J. M (Dolly and Nisa, 2019) 2019	√	√	x	x	x	x	x	x
Huang, B (Huang et al., 2020) 2020	x	√	√	√	x	x	√	√
Tirupal, B (Tirupal et al., 2021) 2020	√	√	√	√	x	√	x	√
Hermessi, H (Hermessi et al., 2021) 2021	√	√	√	√	x	√	x	√
Sebastian, J (Sebastian and King, 2021) 2021	√	√	x	x	x	x	x	x
Diwakar, M (Meher et al., 2019) 2021	x	√	√	√	x	√	x	√
Our work	√	√	√	√	√	√	√	√

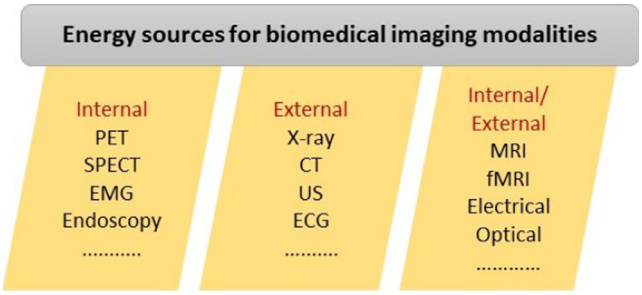

Fig. 2. Energy sources used in medical modalities.

i. The medical imaging modalities, sources of generation, and methods, as shown in Figs. 2 and 3and Table 2.
ii. Comparisons of publicly available online multimodal medical databases and their use in research over the last five years, as shown in Figs. 4 and 5 and Table 3.
iii. Steps used in MMIF, as shown in Fig. 6.
iv. The MMIF techniques in the spatial domain, frequency domain, deep learning, Fuzzy set, sparse representation, and hybrid-based domain, along with their merits and demerits, as shown in Figs. 7–15 and Tables 4 and 5.
v. Different combination of the MMIF, as shown in Fig. 16.
vi. The fusion quality assessment metrics, as illustrated in Tables 6 and 7, and performance analysis of the MMIF techniques using standard datasets, as shown in Figs. 17 and 18 and Table 8.
vii. Current challenges and future directions.

Table 1 shows the prominent reviews articles covered MMIF techniques, modalities, and performance analysis. However, detailed studies on the multimodal databases, research trends in imaging modality grouping, and fusion steps are lacking. Furthermore, current challenges and future directions have not been thoroughly discussed.

The rest of the paper is organized as follows.

Section 2 provides a detailed explanation of the medical imaging modalities. The freely available online multimodal medical databases are discussed in Section 3. The MMIF steps are described in Section 4, and Section 5 describes the MMIF methods in detail. Section 6 illustrates the multimodal medical imaging integration/-combination. Section 7 presents the quality assessment metrics and performance analysis of the MMIF techniques using the same standard database. Section 8 discusses the current challenges and future directions, and Section 9 concludes the review.

2. Medical imaging modalities

Each medical imaging modality has its own information, characteristics, frequencies, and wavelength (Singh et al., 2012). Electromagnetic (EM) waves are randomly scattered, reflected, or absorbed by an object when striking it. The magnetic field produced by the MRIs causes the protons of the body to align. The high-frequency range of X-ray and CT imaging methods, of the order of $3 \times 10^{16} - 3 \times 10^{19}$, renders them extremely radiative and detrimental to human health. On the contrary, the Gamma rays used in the PET and SPECT to detect bioactivity in human organs have higher frequency and less wavelength. The CT, PET, and X-rays are ionization-based, whereas the US and MRI are non-ionization-based (Andreu-Perez et al., 2015). Furthermore, each modality has a unique image acquisition process. The X-ray, CT, and US use internal sources for image acquisition, whereas the PET, SPECT, and EMG use external sources. Some modalities

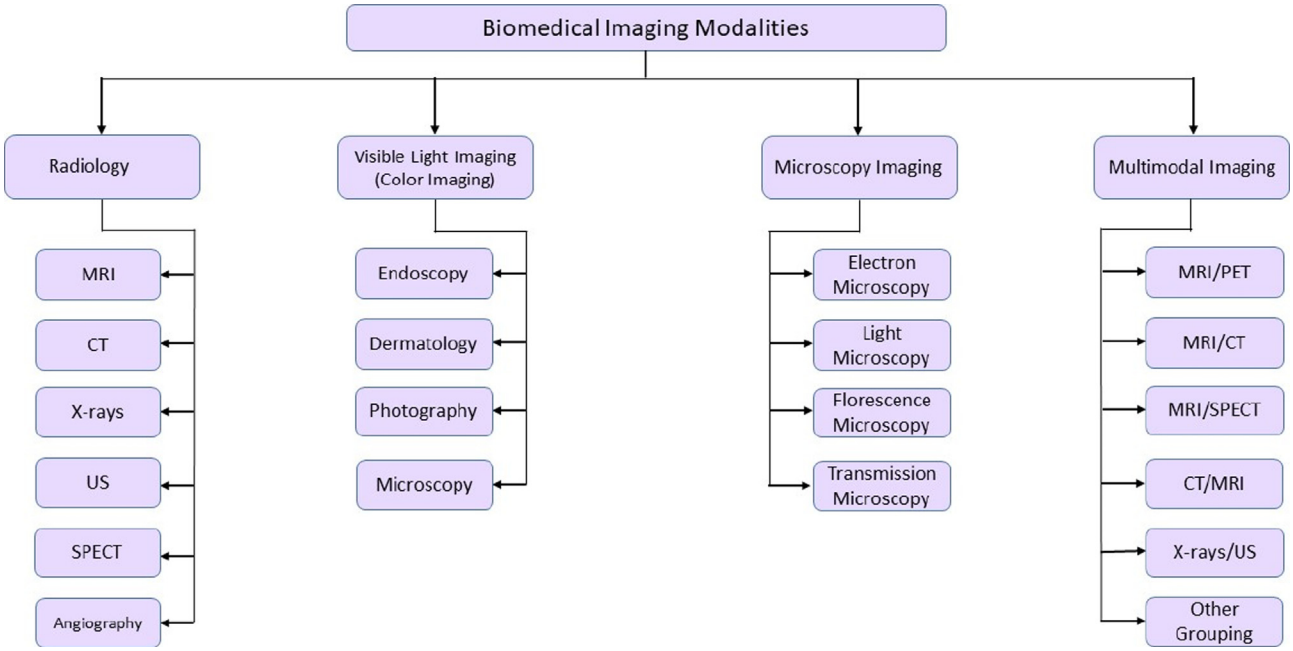

Fig. 3. Detail organization of multimodal medical imaging.

employ hybrid approaches. Fig. 2 depicts the energy sources for medical imaging modalities.

Similarly, invasive and non-invasive techniques are used in medical imaging. Invasive procedures involve injecting an object into the body through an incision or needle injection, whereas non-invasive techniques use radiation, as shown in Table 3.

Each medical imaging modality uses different mechanisms to obtain information, such as radio waves, ionization, and gamma rays. Other techniques include microscopy, visible-light, and multimodal imaging. Fig. 3 shows the detailed organization of medical imaging modalities.

3. Multimodal medical imaging databases

Before delving into MMIF techniques, it is important to understand the multimodal medical image databases and datasets. These databases contain multidirectional medical images acquired from the same patient using different modalities, and are publicly available. Although numerous multimodal medical image databases are available, this study focused on the following six free databases containing thousands of multidirectional medical images acquired using different modalities: The Cancer Imaging Archive (TCIA), Open Access Series of Imaging Studies (OASIS), Alzheimer's Disease Neuroimaging Initiative (ADNI), Whole Brain Atlas (AANLIB), Michigan Institute of Data Science (MIDAS), and Digital Database for Screening Mammography (DDSM). There are other freely accessible online medical imaging databases; however, these databases contain medical images of various organs affected by different diseases. Moreover, medical images can have different formats. Table 3 illustrates the multimodal medical image databases, modality types, body organs, and medical image classifications. Brief introductions to each database are provided below.

3.1. TCIA

TCIA is a cancer image archive. It contains medical images of 22 modalities acquired in the same and different time spans of various organs, and is publicly available. Most of the images are of the chest, brain, and breast organs,witha total of almost 54 different organs (TCIA, 2022). DICOM is the image file format.

3.2. OASIS

It is publicly available neuroimaging dataset containing medical images of five different projects: OAIS-1, OAIS-2, OAIS-3, OAIS-3_TAU, and OAIS-4. OAIS-1 contains416 subjects with 434 sessions, OAIS-2 contains 150 subjects with 373 sessions, and so on. These datasets include both men and women aged 18–96 (Azam et al., 2020). Similarly, the OAIS includes 1379 subjects with 2842 MR Sessions, 2157 PET sessions, and 1472 CT sessions. It also contains the medical images of patients with and without the Alzheimer's disease.

3.3. ADNI

This database contains publicly available medical images of the Alzheimer's disease. Positron emission tomography (PET) and magnetic resonance imaging (MRI) of different body organs are available, and researchers have used these images to test and validate their algorithms (ADNI).

3.4. The whole brain Atlas (AANLIB)

It is a public brain image database provided by the Harvard Medical School. It contains both normal and anomalous brain images. It contains 100 normal brain structures in 2D and 3D formats and images of diseases, such as neoplastic, cerebrovascular, infectious, and degenerative disease (Ramlal et al., 2018; Yang et al., 2016). All the medical images were available in the GIF file format.

3.5. MIDAS

The database contains numerous medical images of various organs. Some are not publicly available, but may be requested (Torrado-Carvajal et al., 2016). All images are in the DICOM and GIF formats.

Table2
Extensively used biomedical imaging modalities comparison.

MMIF imaging modalities	Abbreviation	Method	Attributes
MRI	Magnetic Resonance Imaging	Non-Invasive	Shows anatomical information such as soft tissues, blood flow, Identify brain tumors, dementia and stroke Can't show metabolic information like cancer cell (MITA; Victor and Victor, 2014)
PET	Positron Emission Tomography	Invasive	Shows biochemical changes in pseudo color Shows information about cancer cell (MITA)
CT	Computed Tomography	Non-Invasive	Diagnose bone tumors, fractures, bone disorder, bleeding, stroke etc. Can't show anatomical structures such soft tissues (Andreu-Perez et al., 2015; Du et al., 2016; F. El-Gamal et al., 2016; F. E. Z. A. El-Gamal et al., 2016; Faragallah et al., 2020; Hermessi et al., 2021; Huang et al., 2020; Kaur et al., 2021; Meher et al., 2019; Sebastian and King, 2021; Singh et al., 2012; Tirupal et al., 2021; Dolly and Nisa, 2019; MITA; Victor and Victor, 2014)
X-rays	X-Radiation	Non-Invasive	Provide anatomical structure such as bone crakes, abnormality etc. (Andreu-Perez et al., 2015; Du et al., 2016; F. El-Gamal et al., 2016; F. E. Z. A. El-Gamal et al., 2016; Faragallah et al., 2020; Haidekker, 2013; Hermessi et al., 2021; Huang et al., 2020; James and Dasarathy, 2014; Kaur et al., 2021; Meher et al., 2019; Rajalingam and Priya, 2018; Sebastian and King, 2021; Singh et al., 2012; Tirupal et al., 2021; Dolly and Nisa, 2019; MITA; Victor and Victor, 2014)
SPECT	Single Photon Emission Computed Tomography	Invasive	Diagnose altered blood flow in the brain Information about vascular brain disorders, like moyamoya, Seizure disorders etc.
US	Ultrasound	Non-Invasive	Provide information of inside body using sound waves Also show information of blood flow in vessels (Andreu-Perez et al., 2015; Du et al., 2016; F. El-Gamal et al., 2016; F. E. Z. A. El-Gamal et al., 2016; Faragallah et al., 2020; Hermessi et al., 2021; Huang et al., 2020; Kaur et al., 2021; Meher et al., 2019; Sebastian and King, 2021; Singh et al., 2012; Tirupal et al., 2021; Dolly and Nisa, 2019; MITA; Victor and Victor, 2014)
Endoscopy	–	Invasive	Use of camera to show inside body structure Like examine stomach (O'Mahony et al., 2008)

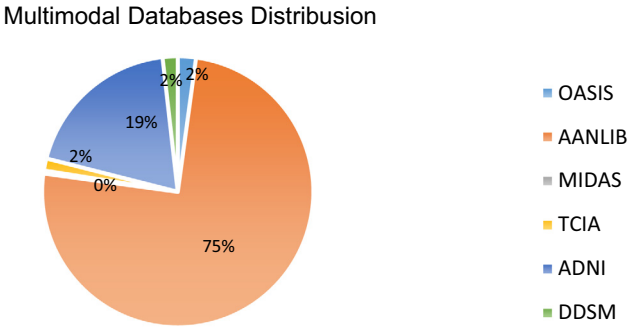

Fig. 4. Frequency distribution of medical image databases.

3.6. DDSM

It contains mammographic images, and is typically used by scientists for mammographic image analysis. It contains images of cases and volumes. A total of 2630 cases are available in 43 volumes (4 views mammography exams). The image file format is 16-bit PGM.

Fig. 4 depicts the use of multimodal databases with the medical image fusion mechanism. The results were obtained from the WoS for the period 2010–2022. Fig. 5 shows the sample images from the Harvard Medical School database (AANLIB).

4. Medical image fusion steps

Image fusion is the process of combining two or more images acquired from the same or different modalities to obtain complementary information of all the images [29–5]. Image fusion rules play an important role in obtaining complementary information from the input images. PET and SPECT are high spatial resolution pseudo-color images, which provide information about soft tissues, blood flow, and metabolism changes in the organs, whereas the MRI, US, CT are low spatial resolution grayscale images, which provide anatomical structure/information of the organs.

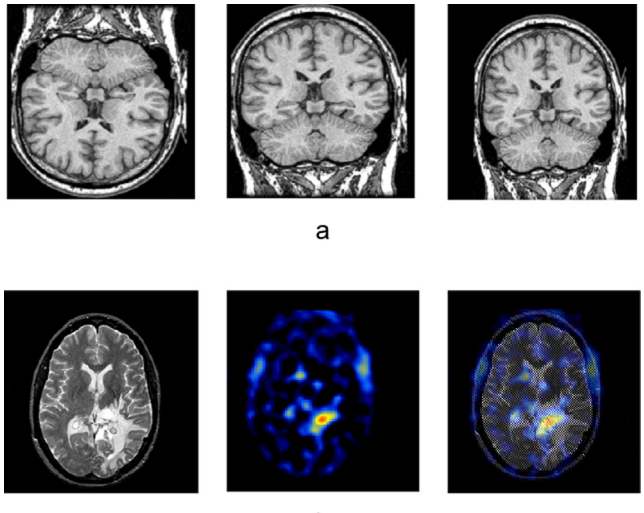

Fig. 5. AANLIB (online free database) (AANLIB, 2020) (a) transaxial, sagittal, and coronal 3D MR brain images,(b) SPECT images with Tumor slice (Khan et al., 2013).

In the MMIF processes, focus must be on the following points:

a. Body organ of interest (such as breast, chest, and brain)
b. Two or more imaging modalities (PET/MRI or MRI/CT)
c. Fusion methods (transform, deep learning, hybrids)
d. Fusion steps/rules

After the fusion process, the final image should not contain: (a) synthetic information, (b) artifacts, such as scratches and dots, or (c) noise or registration issues. Images acquired from the different modalities and same modality with different energy levels may be fused. Fig. 6 shows a graphical representation of the MMIF steps.

The input images are first decomposed to obtain their coefficients using the proper fusion rules. To process the wavelet coefficients, it is important to apply suitable decomposition scales and

Table 3
Multimodal medical image databases.

Database& Online Availability	Modalities Types	Body Organ's	Medical Image Classification & File Format
TCIA 2015	X-rays, MRI, CT, PET, SPECT, Colon etc.	Chest, Brain, Breast, lungs, neck, heart, kidney	Consists of 22 modalities with 54 different organ's and clinical trail's Medical images for normal and different disease of body organ's DICOM file format
OASIS 2010	PET, MRI	Brain	Contains 3059 subjects with MR sessions, 471 PET sessions, and 1472 CT sessions Images in combination of normal, mild, moderate and severe Alzheimer's DICOM file format but can be converted to NIFTI or NRRD format (xxxx; xxxx)
ADNI 2003	PET, MRI, fMRI	Brain	Consists of PET and MRI images for Alzheimer's detection CSV files format
AANLIB 1995	PET, MRI, CT, SPECT	Brain	2D and 3D brain images with normal, Neoplastic disease, Cerebrovascular, Infection disease, and Degenerative disease GIF file format
MIDAS 2010	PET, MRI, CT, US, SPECT etc.	Liver, Heart, Brain, Head, Bones	Contains different modalities medical images acquired at different time spam DICOM and GIF file format
DDSM 1999	X-rays	Breast	Contains 2630 normal and early cancer images with 42–50 μm of resolutions PGN file format

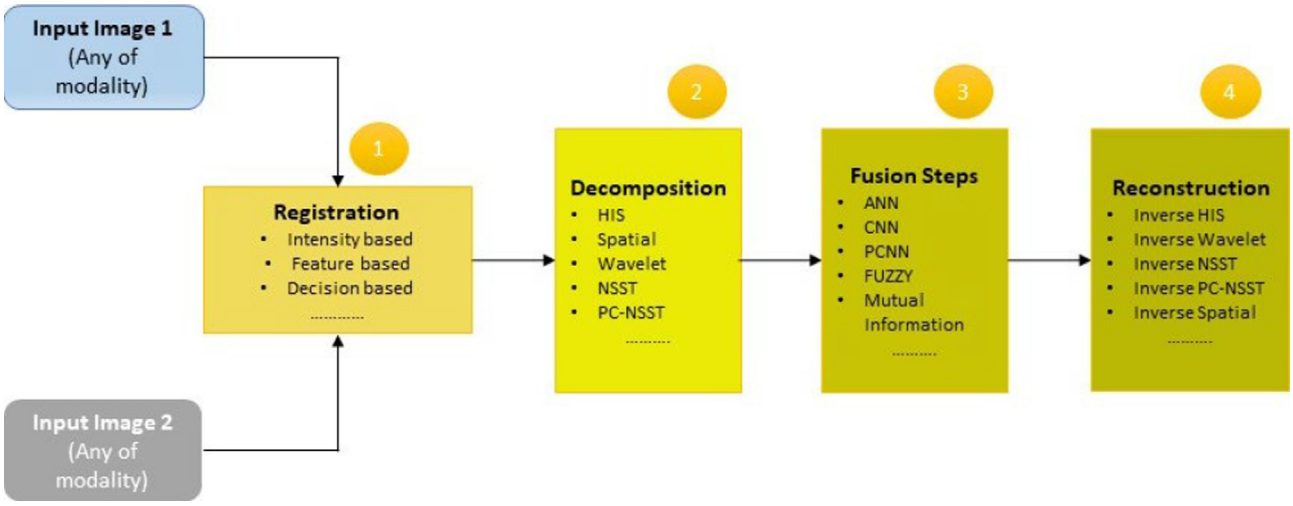

Fig. 6. MMIF image fusion process.

wavelet families. A few scale selections cause loss of image information, whereas too many scale selections cause image blurriness. Two requirements must be met throughout the image fusion process: (1) the fused image must have all relevant medical information that was present in the input images, and (2) it must not contain any new information that was not present in the input images. The researcher determines the body organ of interest first in the multimodal fusion process. Second, choose two or more imaging modalities to fuse using the suitable image fusion method. The fusion algorithm must be validated using performance measures. Subsequently, inverse action is applied to obtain the final fused image (Andreu-Perez et al., 2015; Azam et al., 2020; Du et al., 2016; F. El-Gamal et al., 2016; F. E. Z. A. El-Gamal et al., 2016; Haidekker, 2013; Heba et al., 2017; Hermessi et al., 2021; Huang et al., 2020; Khan et al., 2013; Meher et al., 2019; O'Mahony et al., 2008; Ramlal et al., 2018; Sebastian and King, 2021; Singh et al., 2012; Tirupal et al., 2021; Torrado-Carvajal et al., 2016; Yang et al., 2016; AANLIB; ADNI; Dolly and Nisa, 2019; MITA; TCIA, 2022; Victor and Victor, 2014; xxxx). These steps/rules are applied to obtain complementary information and features to simplify the clinical diagnosis. Image fusion approaches are classified into three types: pixel-level, feature-level, and decision-level. Pixel-level image fusion entails directly combining the original information from the source images or their multi-resolution transformations to produce a final image that is more informative for visual perception. The purpose of feature-level fusion is to extract significant attributes from the original image such as form, length, edges, segments, and orientations. The qualities extracted from the input photographs are combined to form more significant features, resulting in more descriptive and thorough images. A high level of fusion that identifies the true target is referred to as decision-level fusion. It integrates the results of several algorithms to get a final fusion judgment.

Some of the image fusion rules discussed in this study are the principal component analysis (PCA) (Reena Benjamin and Jayasree, 2018), visualization based fusion rules (Tirupal et al., 2019); IFS based cosine similarity (Liu et al., 2018), and consistency verification (Tirupal et al., 2019; Liu et al., 2018; Yang et al., 2014).

4.1. PCA

It is frequently used in the image fusion process to highlight the silent details in the input images. This is used to calculate the weights of the coefficients using the following equations:

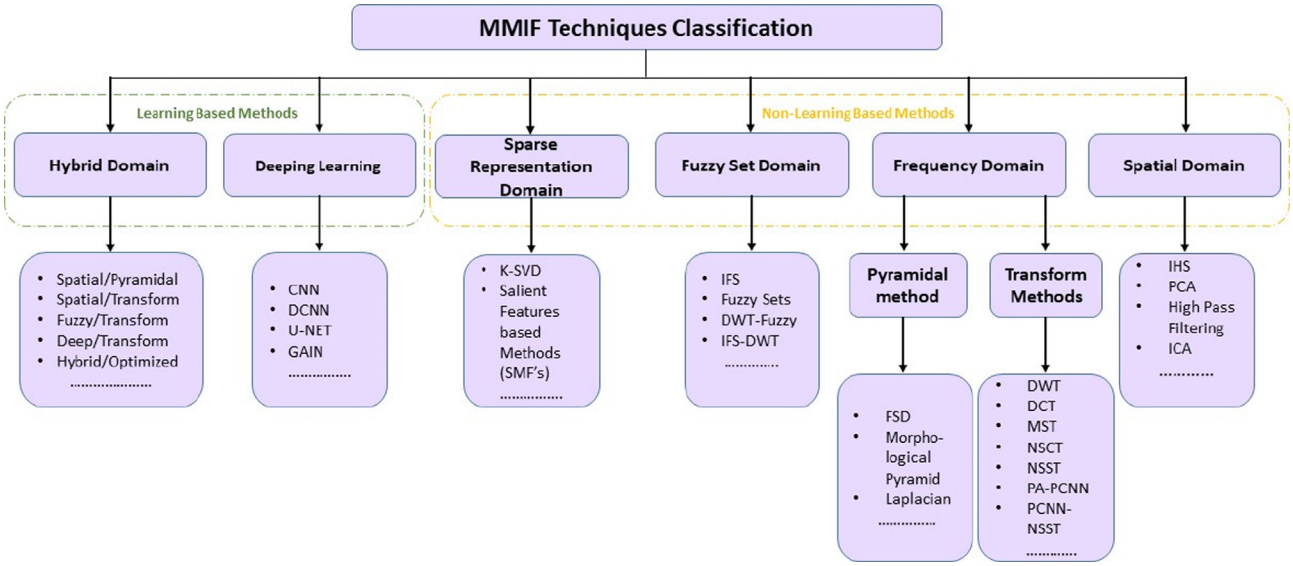

Fig. 7. Classification of MMIF methods.

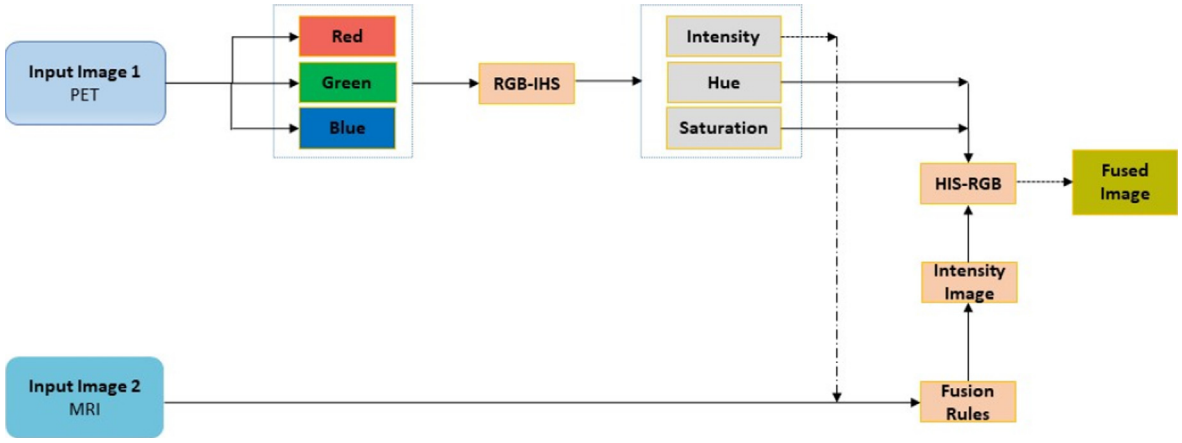

Fig. 8. MMIF using IHS.

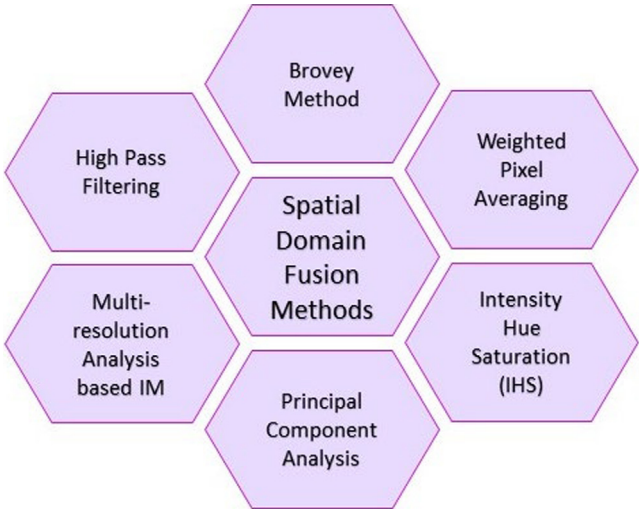

Fig. 9. MMIF methods in spatial domain.

1) Suppose input modalities coefficients are W^1 and W^2

$$W^1 = \begin{bmatrix} z_1^1 \\ z_2^1 \\ z_n^1 \end{bmatrix} W^2 = \begin{bmatrix} z_1^2 \\ z_2^2 \\ z_n^2 \end{bmatrix} \quad (1)$$

2) Covariance matrix measurements

$$CVN\left(W^1, W^2\right) = E[\left(W^1 - \mu_1\right)\left(W^2 - \mu_2\right)] \quad (2)$$

where E denotes expectation vector and μ_1, μ_2 are the coefficients, which can be calculated using Equations (3) and (4).

$$\mu_1 = \frac{1}{n}\sum_{a=1}^{n} Z_i^1 \quad (3)$$

$$\mu_2 = \frac{1}{n}\sum_{a=1}^{n} Z_i^2 \quad (4)$$

Then, the eigen vectors (VCc) and eigen values (Edv) are calculated using Equation (5).

$$[VCcEdv] = eig(CVN) \quad (5)$$

VCc is calculated to obtain normalized weights as:

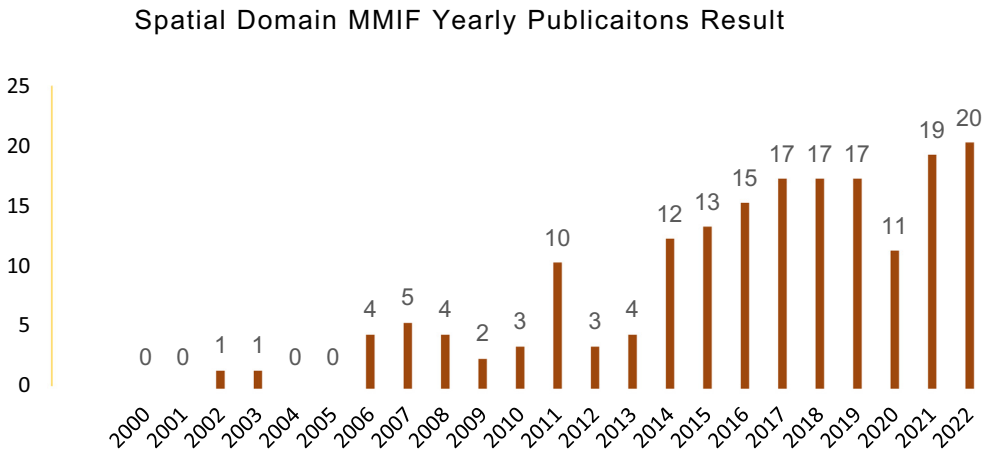

Fig. 10. MMIF publications in spatial domain [WoS 2000–2022].

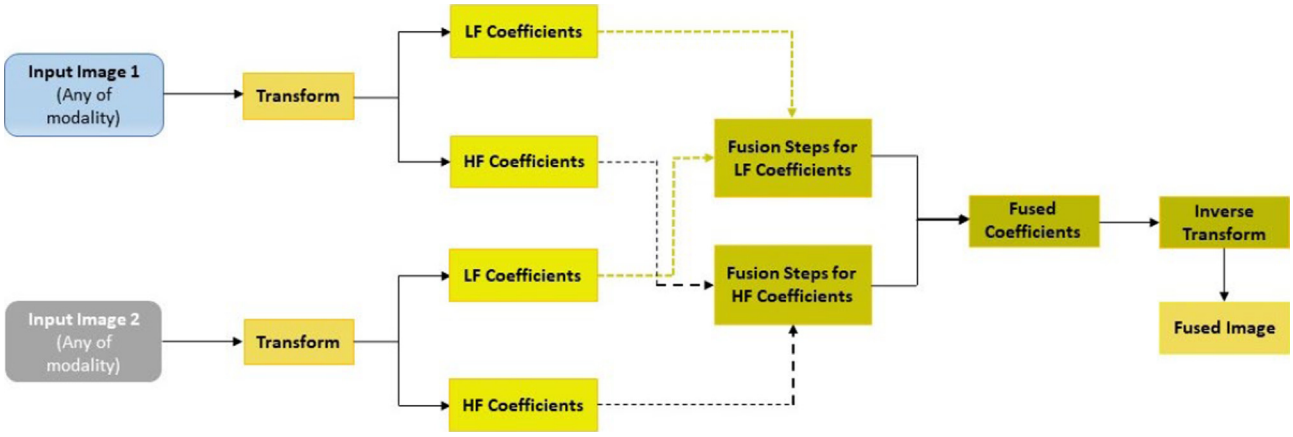

Fig. 11. MMIF structure using transform domain.

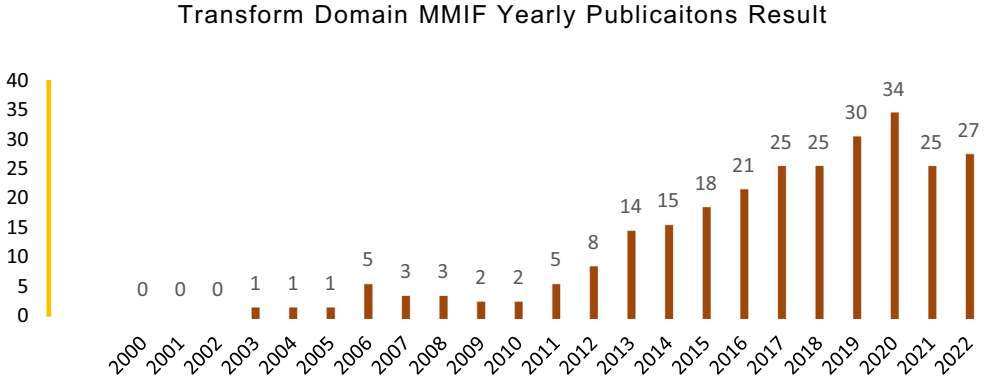

Fig. 12. MMIF publications in Frequency domain [WoS 2000–2022].

$$Ri_1 = \frac{VCc(1)}{\sum\sum VCc}, \; Ri_2 = \frac{VCc(2)}{\sum\sum VCc} \tag{6}$$

Subsequently, the fused coefficient can be calculated as:

$$W_F = W^1 \times Wi_1 + W^2 \times Wi_2 \tag{7}$$

4.2. Visualization based fusion rules

This is used to enhance the contrast of the fused images. This was calculated by subtracting the grey scale values of the image block from the mean values of the block. Contrast visibility (CV) is the best example of visualization-based fusion. This can be stated as:

$$CV = \frac{1}{E \times F} \sum_{(e,f) \in B_k} \frac{|f(e,f) - \mu_k|}{\mu_k} \tag{8}$$

where B_k is the block dimensionality and $\mu_k, |$ and $E \times F$ are mean.

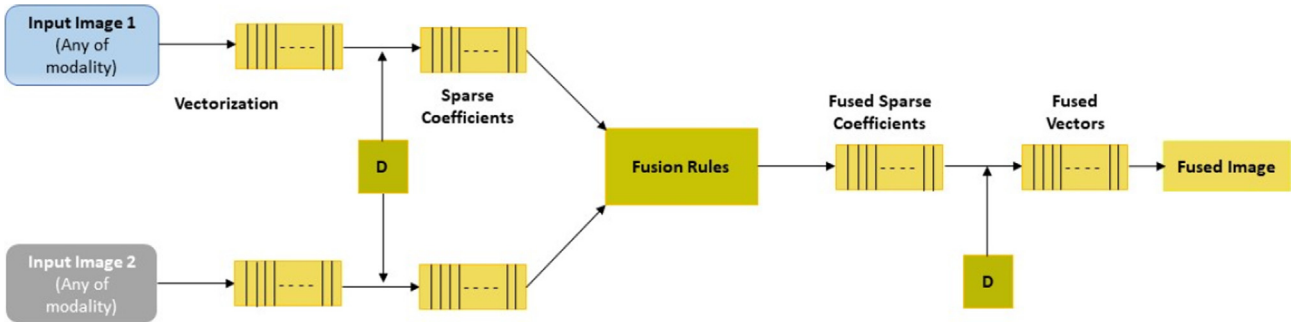

Fig. 13. MMIF structure using SR domain.

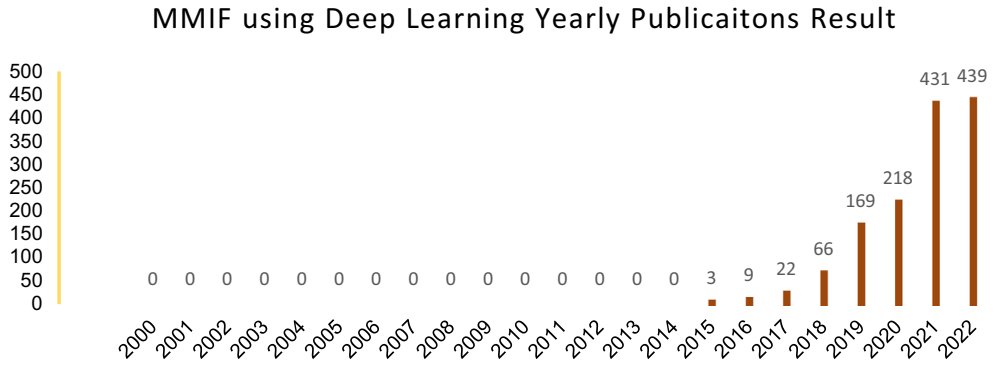

Fig. 14. MMIF publications in DL domain [WoS 2000–2022].

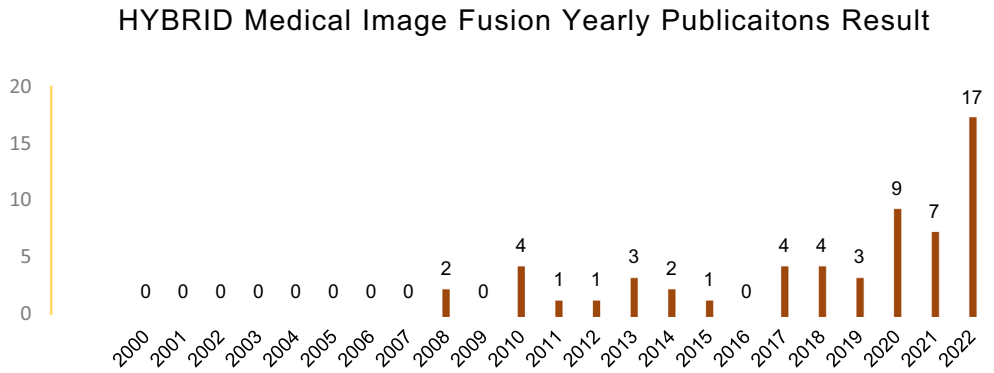

Fig. 15. MMIF publications in Hybrid domain [WoS 2000–2022].

4.3. IFS based cosine similarity

It is used to improve the features of the fused image by calculating the cosine similarity of the input images. This can be calculated as (Haribabu et al., 2023):

$$CS_{IFS}(G,H)\frac{1}{n}\sum_{j=1}^{n}\frac{\mu_G(C_j)\mu_H(C_j)+V_G(C_j)V_H(C_j)}{\sqrt{\mu_G^2(C_j)+V_G^2(C_j)}\sqrt{\mu_H^2(C_j)+V_H^2(C_j)}} \quad (9)$$

4.4. Consistency verification

This is a fusion rule used to reduce errors/incorrect pixel values. A window size of 7X7 was applied to generate a new mapping window for decision-making purposes.

5. Multimodal image fusion techniaues

This section provides an in-depth overview of MMIF methods, focusing on six dimensions. Fig. 7 depicts the MMIF technique classification along with the most familiar methods.

i. Spatial domain
ii. Frequency domain (Transform and Pyramid)
iii. Fuzzy set domain
iv. Deep learning domain
v. Sparse representation, and
vi. Hybrid domain

Three types of operations were performed using all the MMIF methods (Meher et al., 2019; Narsaiah et al., 2018).

i. Pixel level: based on the pixel combinations of all the images

Table 4
MMIF methods classification.

Research Studies and publication year	Fusion Domain	Modalities Combination	MMIF Methods	Database
R. Stokking et al. (Stokking et al., 2001) 2001	Spatial	SPECT/MRI	HSV	AANLIB
C. He et al. (He et al., 2010) 2010		PET/MRI	IHS - PCA	AANLIB
R. Bashir et al. (Bashir et al., 2019) 2019		CT/X-ray/MRI/SPECT	SWT - PCA	AANLIB
Z. Fu et al. (Fu et al., 2020) 2020		MRI/CT	Gradient Filtering	AANLIB
Y. Yang et al. (Yang et al., 2010) 2010	Frequency	MRI/CT	Coefficients processing using visibility and variance based schemes	AANLIB
S. Das, & M.K. Kundu (Das and Kundu, 2013) 2013		CT/MRI, T1_W_MR/MRA, FDG_PET/MR	NSCT-RPCNN	AANLIB
B.R. Kumar (Kumar, 2014) 2013		CT/MRI, MRI T1/T2	NSCT	AANLIB
P. SGomathi&B. Kalaavathi (Gomathi and Kalaavathi, 2014) 2014		MRI/SPECT, CT/MRI	Redundant Wavelet Transform – Maximum selection rules	AANLIB
G. Yang et al. (Yang et al., 2015) 2015		CT/MRI, MRI/PET, and MRI/SPECT	NSCT-Generalized Gaussian Density	AANLIB
M. Yin et al. (Singh et al., 2015) 2018		CT/PET/MRI	NSST-PAPCNN	ADNI
M. Arif, &G. Wang (Arif and Wang, 2020) 2019		MRI/MRA	FCT via Genetic Algorithm	AANLIB
S. Polinati, &R. Dhuli (Polinati and Dhuli, 2020) 2020		SPECT/MRI/PET	Empirical Wavelet Decomposition	AANLIB
Q. Hu et al. (Hu et al., 2020) 2020		MRI/CT	NSCT-Gabor filtering along with dictionary learning	AANLIB
K. T. Atanasov (Atanassov, 1994) 1986	Fuzzy Set	MRI/CT	IFS	AANLIB
W. Z. Ismail, &K. S. Sim (Ismail and Sim, 2011) 2011		MRI/CT	**Contrast Enhancement Dynamic Histogram Equalization**	ADNI
Sanjay AR et al. (Sanjay et al., 2017) 2017		CT/MRI-T2, MRI-FLAIR	Discrete Wavelet Transform and Type-2 Fuzzy Logic	AANLIB/ADNI
Aysha S, Tirupal T. (Aysha) 2016		MRI/CT	yager's intuitionistic fuzzy sets	image fusion toolbox (ver 1.0)
Tirupal T et al. (Tirupal et al., 2017) 2017		MRI/CT	Sugeno's intuitionistic fuzzy set- entropy calculates the optimum values of membership	AANLIB
B. K. S. Kumar (Shreyamsha Kumar, 2015) 2015	Sparse Representation	Multisensory MRI	DWT-Cross Bilateral Filter (CBF)	Imagefusion.org
D. P. Bavirisetti (Bavirisetti et al., 2017) 2017		MRI/CT	Guided Image Filter-Structure Transferring Filter-Gradient Preserving Filtering	AANLIB
L. Jian (Jian et al., 2018) 2018		MRI/CT	Rolling Guidance Filter (RGF) and Joint bilateral filter	Imagefusion.org
] S. Maqsood, U. Javed (Maqsood and Javed, 2020) 2019		MRI/CT	Sparse Representation-Multiscale decomposition	AANLIB
Y. Liu et al. (Liu et al., 2020) 2020		MRI/CT	Joint Sparse Representation	AANLIB
Y.P. Wang et al. (Wang et al., 2007) 2007	Deep Learning	MRI/CT	fuzzy radial basis function neural networks	AANLIB
Z. Wang, Y. Ma (Wang and Ma, 2008) 2008		MRI/CT	M−PCNN	AANLIB
J. Teng et al. (Teng et al., 2010) 2010		MRI/CT/SPECT	Neuro Fuzzy method with mixes BP algorithm and least mean square (LMS) algorithm	AANLIB
S. Sivasangumani (Sivasangumani et al., 2015) 2015		MRI/CT	RFC-PCNN	AANLIB
H. Hermessi (Hermessi et al., 2018)		MRI/CT	Similarity learning in the shearlet domain	AANLIB

Table 4 (*continued*)

Research Studies and publication year	Fusion Domain	Modalities Combination	MMIF Methods	Database
2018				
X. Liang et al. (Liang et al., 2019) 2019		MRI/PET	Multi-layer concatenation fusion network (MCFNet)	AANLIB
R. Hou et al. (Hou et al., 2019) 2019		MRI/CT	CNN-dual-channel spiking cortical model in NSST domain	AANLIB
F. Fan et al. (Fan et al., 2019) 2019		CT/MR-T2	W-Net (FW-Net) method	AANLIB
R. NandhiniAbirami (Nandhini Abirami et al., 2022) 2022		MRI/PET	GAN Model	AANLIB
S. Daneshvar, H. Ghassemian (Daneshvar and Ghassemian, 2010) 2010	Hybrid	MRI/PET	HIS-RIM	AANLIB
S. Das, M.K. Kundu (Das and Kundu, 2012) 2012		CT/MRI	PCNN in NSCT domain	AANLIB
K. Sharmilaet al.(Sharmila et al., 2013) 2013		CT/MRI	Discrete Wavelet Transform-Averaging-Entropy-Principle Component Analysis method [DWT-A-EN-PCA]	AANLIB
C.T. Kavitha, C. Chellamuthu (Vickers, 2017) 2014		PET/MTI/SPECT	Swarm Intelligence-NN	AANLIB
S.D. Ramlal et al. (Ramlal et al., 2019) 2019		CT/MRI	SWT in NSCT domain	AANLIB
L. Xu et al. (Xu et al., 2020) 2020		CT/MRI/SPECT	DWT-Homomorphic Filter	AANLIB
G. Hawna et al. (Goyal et al., 2022) 2022		CT/MRI	CBF-Domain Transform Filter-RGB	AANLIB

ii. Feature level: region-based methods are used to extract the image features
iii. Decision level: based on region detection and classification of object

MMIF based on the spatial domain was a popular topic in early research. In this method, fusion rules are applied to the input image pixels to obtain a fused image. However, owing to the issues of low signal-to-noise ratio (SNR) and spatial and spectral distortion, research interest in MMIF in the spatial domain has gradually declined in recent years. Intensity hue saturation (IHS), high-pass filtering, maximum/minimum selection methods, and PCA are examples of spatial-domain MMIF techniques. In the frequency domain, the input images are first transformed into the frequency domain, then fusion rules are applied. Finally, an inverse transformation is applied to obtain the fused image. They are further categorized into the transform and pyramidal domains (Azam et al., 2021).The Fuzzy set domain is adequate for avoiding vagueness in the input images. However, dealing with uncertainty remains challenging. Recently, deep learning has emerged as a new area of research in medical image fusion. The Convolution Neural Network (CNN), U-Net, and Generative Adversarial Network (GAN) are the typical models used for medical image fusion. Sparse representations and hybrid domains are also prominent areas of MMIF. This section provides a brief overview of the MMIF domains.

5.1. Spatial doman methods

In the spatial-domain methods, fusion is performed on a pixel basis. IHS, PCA Brovey, high-pass filtering, and ICA methods are widely used in the spatial domain (El-Gamal et al., 2016).The IHS method converts an RGB image into IHS components. The fused images are obtained by transforming the IHS and RGB images. The IHS method performs efficiently in terms of color visualization (Subramanian et al., 2015). Fig. 8 illustrates the IHS method diagrammatically. The HSV method proposed in (Stokking et al., 2001) fused MRI and SPECT images using a color-encoding mechanism. This provides better structural and metabolic features with less spectral distortion. Similarly, the fusion method proposed in (He et al., 2010) merges the features of the IHS with those of the PCA and obtains acceptable results. The resulting image has high spatial information and reduced spectral distortion. However, this method has an image-registration problem. A combination of the PCA and SWT method was proposed in (Bashir et al., 2019) and achieved better results than that with the IHS and ICA. The research interest in the spatial domain has gradually decreased because of spectral and spatial distortion issues. Figs. 9 and 10 depicts the spatial domain methods and publication results of the MMIF methods in the spatial domain. The results were obtained from the Web of Science (WoS).). Spatial domain methods are simpler, faster to compute, and provide better color visualization. However, these methods have been unsuccessful in real-world scenarios. The fused image exhibited spectral distortion and sharpening issues.

5.2. Frequency domain methods

In frequency-domain methods, a Fourier Transform (FT) is applied to convert the input medical images into frequencies or other domains. Fusion rules are then applied to the resulting image, followed by an inverse FT to obtain the final fused image (Princess et al., 2014). Frequency-domain methods are divided into the pyramid and transform domain (Parmar and Kher, 2012).

The pyramid-based image-fusion methods are used to improve the spectral information in the final fused image (Du et al., 2016; Krishnamoorthy and Soman, 2010). In pyramid transform, the detail of the fused image depends on the decomposition levels, i.e., the scales and proper family selection. The Laplacian pyramid

Table 5
MMIF domains comparison.

Domain	Advantages	Limitations
Spatial	• Pixel level fusion • Simplest and faster computation • Low complexity • Better color visualization (Mishra and Palkar, 2015; Bhat and Koundal, 2021)	• Fused image has sharpening issue • Spectral distortion and less visual quality • Edges smoothness and low contrast issues (Mishra and Palkar, 2015; Bhat and Koundal, 2021)
Frequency	• Less distortion of spectral details than Spatial domain • Multiscale Transform Theory • High Signal to Noise Ratio (SNR) than Spatial domain methods • With good edges information and good visual quality of fused image (Huang et al., 2020; Masood et al., 2017; Sharma et al., 2020)	• Spatial details are missing • Complex than Spatial domain process • Defects of activity level measurements • Image registration issues (Huang et al., 2020; Masood et al., 2017; Sharma et al., 2020)
Fuzzy	• Fused image with less spectral distortion • Good visual quality • Less blocking effects • More detail edges (Li and Yin, 2011; Bavirisetti et al., 2017)	• Spatial distortion • Image registration problem • Uncertainties • Localization problems (Li and Yin, 2011; Bavirisetti et al., 2017)
Sparse Representation	• More detail edges • Better visual quality • Good contrast • Extract enough features (Bavirisetti et al., 2017; Bhat and Koundal, 2021)	• Edge distortion issue • Image registration problem • Fused image has artifacts (Bavirisetti et al., 2017; Bhat and Koundal, 2021)
Deep Learning	• Better image optimization • Good performance on large input data • Effective to extract information from dark regions • Flexibility in customization (Bhat and Koundal, 2021)	• Semantic loss issue • Convergence and overfitting problems (Bhat and Koundal, 2021)
Hybrid	• Extract features detail • Good contrast and smooth edges • Less artifacts (Atrey et al., 2010)	• Non-uniformity • High Complexity • Difficult to train large datasets (Atrey et al., 2010)

proposed in (Du et al., 2016) is one of the widely used methods, which employs a multi-scale decomposition process to obtain the coefficients. These coefficients are then fused using the weighted fusion method, followed by an inverse Laplacian. However, this method suffers from visualization problems. Pyramid transform methods include the morphological pyramid, slope pyramid, and filter subtract decimate (FSD) method (Krishnamoorthy and Soman, 2010; Sadjadi, 2005).

Transform-domain methods use a multi-resolution approach to increase the accuracy of fused images. The transform domain methods employ a three-step procedure. First, the input images are decomposed into low- and high-frequency sub-bands. In the second step, multiple fusion rules are applied to these coefficients/sub-bands to obtain the fused coefficients, and an inverse operation is performed to obtain the final fused image. Fig. 11 depicts the transform-based MMIF process. The wavelet transform (WT) is the most commonly used method in the transform domain. There are other methods, such as the discrete wavelet transform (DWT), curvelet transform (CT), dual tree complex wavelet transform (DT-CWT), non-subsampled contourlet transform (NSCT), and non-subsampled shealet transform (NSST) (Yang et al., 2010; Das and Kundu, 2013; Zarif et al., 2014). The WT method performs better at preserving the spectral and spatial information using the localization mechanism. However, the down-sampling process fails to satisfy the shift-invariant condition. To overcome this problem, the redundant discrete wavelet transform (RDWT) was proposed in (Gomathi and Kalaavathi, 2014), which performed better in terms of component information. However, this method failed to obtain edge information. To address the shortcomings of scalar wavelets, the multi-wavelet transform (MWT) was proposed in (Wang, 2004). The MWT provides better fusion results. However, the edge smoothness remains an issue. The DT-CWT method was proposed in (El-Hoseny et al., 2018) based on the histogram matching followed by an optimization algorithm, and it provided better results than the DWT-based fusion methods. However, the contour and edge smoothness issues remain unresolved. A CT-based image was proposed in (Yang et al., 2008), which improved the localization problem but could not solve the problems of the WT and its alignment methods.

In (Kumar, 2014); the MMIF technique based on directive contrast in the NSCT domain was proposed, which provided superior fused results in terms of color distortion compared to the DWT, DT-CWT, and Daubechies complex wavelet transform (DCxWT). In (Yang et al., 2015), statistical measurements based on the MMIF in the NSCT domain were proposed, where weighted maps and entropy functions were applied to the high- and low-frequency coefficients. This method provided the maximum number of salient features. Similarly, an enhanced contrasting MMIF method for the NSCT domain was proposed in (Bhatnagar et al., 2015). In this method, the modified Laplacian and weighted matrix methods were used during the image decomposition phase to extract the edge information. This method outperforms the DWT, NSCT, and CONT methods and provides maximum structural information. The most familiar methods, such as the ST and NSST, were proposed in (Biswas and Sen, 2019; Xiaoxue et al., 2015; Yin et al., 2018) for the MMIF, providing multi-directional details and less spectral and spatial distortions than the NSCT. A parameter adaptive pulse-coupled neural network (PA-PCNN) in the NSST domain was presented in (Singh et al., 2015). The PA-PCNN was used in this method to fuse the high-frequency coefficients, whereas the energy preservation function was used to fuse the low-frequency coefficients. Inverse NSST was applied to obtain the final fused image. Fig. 12 shows the publication results of the MMIF methods in the transform domain. The results were obtained from the Web of Science (WoS). The frequency-domain methods overcome the issue of spectral distortion and achieve high SSIM values with good edge information. However, the final fused image using the frequency domain has less spatial detail, and activity-level measurements are difficult (Huang et al., 2020; Mishra and Palkar, 2015; Bhat and Koundal, 2021).

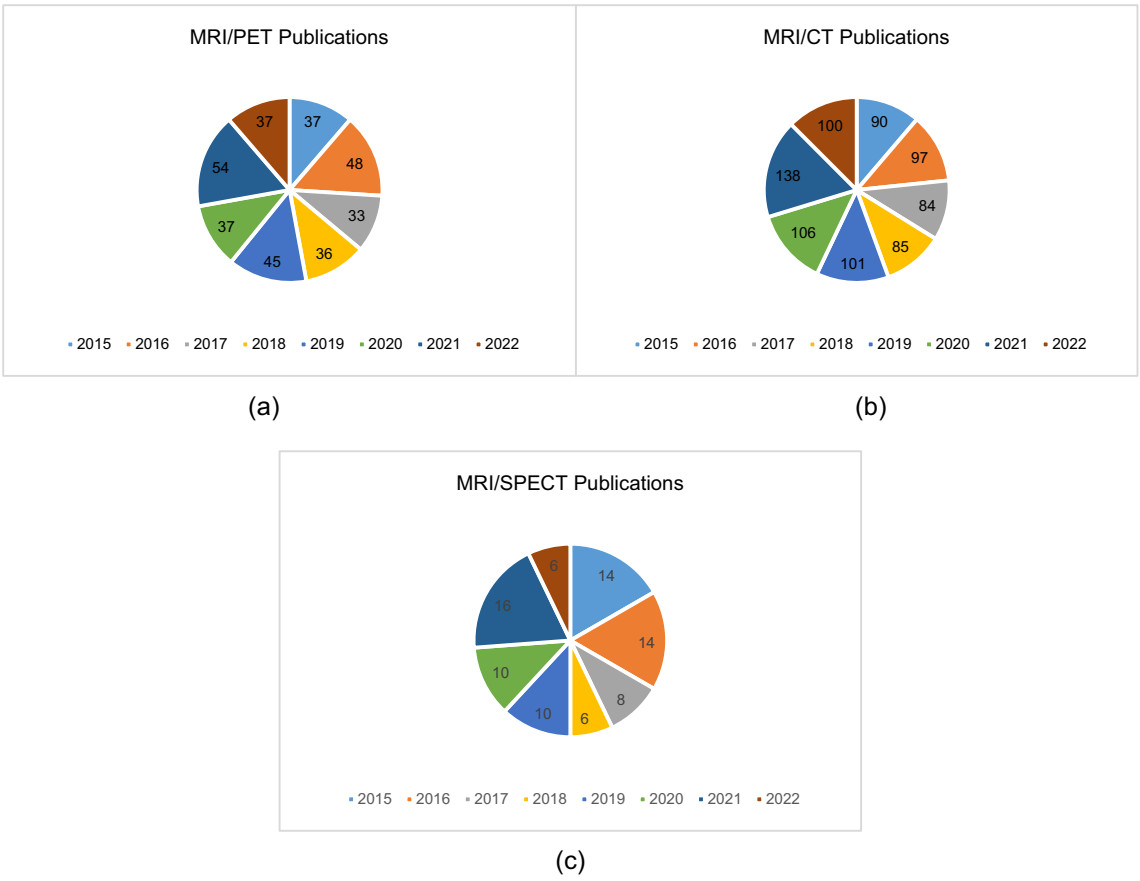

Fig. 16. Research trends towards modalities integration [WoS 2015–2022]. (a) PET/MRI medical image fusion publications, (b) PET/CT medical image fusion publications, (c) PET/MRI medical image fusion publications (Statistical timeframe 2015–2022).

5.3. Fuzzy set domain

In the MMIF methods, acceptable color visualization, minimum spectral and spatial distortion, and edge smoothness and enhancement are vital for assisting in clinical diagnosis. Various methods, such as the gray-level transform, histogram, and gray-level grouping are available in the literature (Ismail and Sim, 2011; Maini and Aggarwal, 2010). However, these methods do not provide the necessary MMIF information. A Fuzzy-set mathematical tool was proposed to overcome the vagueness in the fused image. However, image registration and uncertainty remain as issues. Intuitionistic Fuzzy-set (IFS) presented in (Atanassov, 1994) is a generalized version of the Fuzzy set method; however, it reflects high uncertainty. Another method-based on the DWT and Fuzzy logic was proposed in (Sanjay et al., 2017), wherein averaging rules were used to obtain the high-frequency coefficients, and Fuzzy-logic-based methods were used to obtain the low-frequency coefficients. This method overcomes the problem of uncertainty. The MMIF method based on the IFS proposed in (Aysha) provided better results in terms of uncertainties than the non-Fuzzy methods. The IFS-DWT was presented in (Tirupal et al., 2017), which enhanced the MMIF-fused images in terms of color visualization and fewer uncertainties. The Fuzzy domain methods performed well, and the fused images exhibited less spectral distortion, better visual quality, and extracted detailed features. However, these methods involve image registration, optimization, and overfitting issues (Li and Yin, 2011; Bavirisetti et al., 2017; Bhat and Koundal, 2021).

5.4. Sparse representation domain

Sparse representation (SR) is a powerful tool for better understanding the human visual system and is used in many areas, such as facial expression detection, object tracking and occlusion, and image fusion (Li and Yin, 2011). Fig. 13 graphically illustrates the MMIF process in the SR domain. The steps are described as follows.

a. Sliding window is used to transform the input medical images into vectors form.
b. An over complete dictionary (D) is added to the transform vector to obtain the sparse coefficients.
c. Fusion rules are applied to obtain fused sparse coefficients.
d. An over-complete dictionary (D) is applied to the fused sparse coefficients to obtain the fused vectors.
e. Reverse Step (a) to obtain the final fused image.

Two steps can be used to create a dictionary (D): fixed-based and learning-based. The k-SVD method is one of the best examples of (D) and uses a learning-based method. The learning-based method performed better than the fixed-based method. The MMIF methods based on the SR domain (Li and Yin, 2011) have persistent contrast and edge-distortion issues. Researchers have proposed several combinations of SR structures to obtain a fused image with more color, spectral, and spatial information.

Salient feature methods (SFMs) differ significantly from the other MMIF methods as they have many advantages over the other MMIF methods, such as shift invariance, simplicity, and efficiency in extracting the silent features. Edge preservation is vital in the MMIF methods. Several edge filtering methods, such as the guided

Table 6
MMIF Objective method performance assessment metrics with a reference image.

Statistical Parameter	Abbreviation	Formula	Description	Ref.
CC	Cross-Correlation	$CC = \frac{\sum_{i=1}^{I}\sum_{j=1}^{J}[(IMG_r(i,j)-\bar{IMG_r}).(IMG_f(i,j)-\bar{IMG_f})]}{\sqrt{\sum_{i=1}^{I}\sum_{j=1}^{J}[\left(IMG_r(i,j)-\bar{IMG_r}\right)]\sum_{i=1}^{I}\sum_{j=1}^{J}[\left(IMG_f(i,j)-\bar{IMG_f}\right)]}}$	Computes spectral features of similarity. Higher the CC value means better results	(Yang et al., 2008)
mi	Mutual Information	$MI_{IMG_r,IMG_f} = \sum_{i=1}^{I}\sum_{j=1}^{J} J_{IMGrIMG_f}(i,j)\log_2\left[\frac{i_{IMG_r,IMG_f}(i,j)}{j_{IMG_r}(i,j)j_{IMG_f}(i,j)}\right]$ $MI = MI_{IMG_1IMG_f} + MI_{IMG_2IMG_f}$	Computes dependency levels. The higher the MI value means better fusion	(Haddadpour et al., 2017)
OP	Overall Performance	$OP = \frac{\sum_{a=1}^{3}(D_k - AG_a)}{3}$, a = RGB Where AG is Average Gradient & D is the discrepancy.	Computes deviation between the gradient and discrepancy. The higher the OP value means better fusion	(Nandhini Abirami et al., 2022)
SIMM	Structure Similarity Index measures	$SSIM = \frac{\left[2\mu_{IMG_{or}}\mu_{IMG_{fsd}} + c_1\right]\left[2\sigma_{IMG_{or}IMG_{fsd}} + c_2\right]}{\left[\mu^2_{IMGo_r} + \mu^2_{IMG_{fsd}} + c_1\right]\left[\sigma^2_{IMG_{or}} + \sigma^2_{IMG_{fsd}} + c_2\right]}$	Computes the similarities between original and fused image. The higher the SSIM value means better fusion	(Fan et al., 2019)
MAE	mean absolute error	$MAE = \frac{1}{M \times FSD}\sum_{m=1}^{M}\sum_{fsd=1}^{FSD}\lvert IMA\rvert GM_{or}(m,fsd) - IMG_{fsd}(m,fsd)\rvert$	Computes the errors between original and fused image	(Sanjay et al., 2017)
PSNR	peak signal to noise ratio	$PSNR = \frac{(255)^2}{\frac{1}{M\times FSD}\sum_{m=1}^{M}\sum_{fsd=1}^{FSD}(IMG_{or}(m,fsd) - IMG_{fsd}(m,fsd))^2}$	Computes intensity levels between original and fused image. The higher the PSNR value means better fusion	(Balasubramaniam and Ananthi, 2014)
DIV	difference invariance	$DIV = \frac{\sigma_r^2 - \sigma_f^2}{\sigma_r^2}$	Computes the variation between original and fused image	(Mhangara et al., 2020)
SC	structural content	$SC = \frac{\sum_{g=1}^{G}\sum_{h=1}^{H}(IMG_r(g,h))^2}{\sum_{g=1}^{G}\sum_{h=1}^{H}(IMG_f(g,h))^2}$	Computes the strength of the fused image. SC value must be high	(Memon et al., 2015)
AD	average difference	$AD = \frac{1}{M \times FSD}\sum_{m=1}^{M}\sum_{fsd=1}^{FSD}(IMG_{or}(m,fsd) - IMG_{fsd}(m,fsd)$	Computes the difference between original and fused image	(Memon et al., 2015)

Table 7
MMIF Objective method performance assessment metrics without a reference image.

Statistical Parameter	Abbreviation	Formula	Description	Ref.
FMI	Functional Mutual Information	$FMI = MI_{Img_1Img_{fsd}} + MI_{Iimg_2Img_{fsd}}$	Computes the degree of dependency between source and fused image Higher the FMI value means better results	(Mhangara et al., 2020)
FS	Fusion Symmetry	$FS = abs\left[\frac{Img_{XFSD}}{Img_{SFSD} + Img_{YFSD}} - 0.5\right]$	FS shows symmetry information in fused image. The lower the MI value means better fusion	(Zhang et al., 2012)
M	Mean	$M = \frac{1}{I\times J}\sum_{i=1}^{I}\sum_{j=1}^{J} IMG_{fsd}(i,j)$	Computes average value. The higher the M value means better fusion	(Atrey et al., 2010)
FF	Fusion Factor	$FF = Img_{XFSD} + Img_{YFSD}$	Computes the fusion factors. It must be high	(Singh and Khare, 2014)
SD	Standard Deviation	$SD = \sqrt{\frac{\sum_{i=1}^{Q}\frac{\sum_{j=1}^{R}(f(i,j)-u)^2}{QR}}{}}$	Computesintensity variationof the fused image. It must be high for better fusion	(Wang and Chang, 2011)
EN	Entropy	$EN = -\sum_{I=0}^{L-1} P_i log P_i$	Computesthe information quantity in fused image. EN must be high for better fusion	(Haddadpour et al., 2017)
FI	Fused Index	$FI = \frac{MIImg_{XFSD}}{MIImg_{YFSD}}$	Computes the degree of symmetry information in fused image	(Singh and Khare, 2014)
SCD	Sum of Correlation Difference	$SCD = corl2(fsd - img\_1, img\_2) + corl2(fsd - img\_2, img\_1)$	Computes the transmitted information from source to fused image. SCD value must be high	(Liu et al., 2018)

filter (GF), cross bilateral filter (BF), and rolling guided filter (RGF), play a significant role in image fusion (Bavirisetti et al., 2017; Shreyamsha Kumar, 2015; Jian et al., 2018). SFM methods are now used as preprocessing tools in the MMIF process to increase the contrast and reduce noise. Equations (10)–(13) describe the edge-preserving image fusion filters.

$$BLYR_i^1 = A_1 * EF_i$$

$$BLYR_i^2 = B_2 * EF_i \tag{10}$$

$$DLYR_i^1 = A_1 - BLYR_i^1$$

$$DLYR_i^2 = - * BL_i^2 \tag{11}$$

where *BLYR* and *DLYR* denote the base and detail layers, respectively, *A* and *B* represent the input images, and *EF* is an edge-

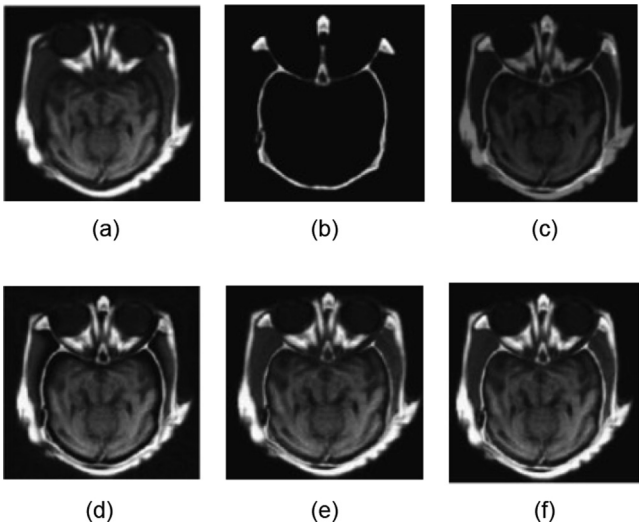

Fig. 17. Qualitative results for MRI/CT images [AANLIB]. (a) MRI image, (b) CT image, (c) NSCT, (d) NSST-PAPCNN, (e) IFCNN, (f) N-Fuzzy.

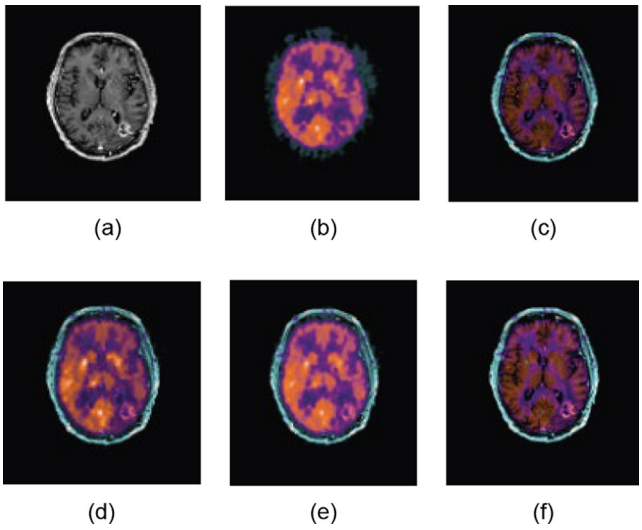

Fig. 18. Qualitative results for MRI/PET images [AANLIB]. (a) MRI image, (b) PET image, (c) NSCT,(d) NSST-PAPCNN, (e) IFCNN, (f) N-Fuzzy.

preserving filter. Subsequently, both the layers can be fused using the fusion rules given in the following equation:

$$BLYRfsd = fsdB\left(BLYR_i^1, BLYR_i^2\right)$$

$$DLYRfsd = fsdD\left(DLYR_i^1, DLYR_i^2\right) \quad (12)$$

where *BLYRfsd* and *DLYRfsd* denote the fused base and detail layers, respectively, and *fsdB* and *fsdD* are the fusion rules. Finally, we obtain a fused image using Equation (13).

$$Imgfsd = BLYRfsd + DLYRfsd \quad (13)$$

The SR domain methods performed well, and the fused images exhibited less spectral distortion, better visual quality, and extracted detailed features. However, these methods involve image registration, optimization, and overfitting issues (Li and Yin, 2011; Bavirisetti et al., 2017; Bhat and Koundal, 2021).

5.5. Deep learning domain

Recently, deep learning (DL) has emerged as a rapidly expanding field in the MMIF research. DL techniques comprise multiple layers, each of which receives an input from the previous layer (Zhou et al., 2019). DL methods include the CNN, deep convolution neural networks (DCNSs), U-Networks, and GAN. The most common deep learning model is the CNN (Krizhevsky et al., 2017). To overcome the issues of feature extraction, edge smoothness, spectral and spatial distortions, and fusion rules, the CNN model was first applied to the MMIF in 2017 and produced promising results compared to the other domain image fusion methods (Liu et al., 2017). CNN's are capable of recognizing and classifying the features, and are widely used to analyze the visual characteristics of images. A CNN comprises features/convolutions, pooling, and fully connected layers. The CNN complexity increases from layer to layer to identify the maximum features of the image. However, issues in the CNN include the requirement of annotated datasets, time-consuming dataset training, complexity in convergence, and repeated adjustment of overfitting. The MCFNet method presented in (Liang et al., 2019) solves the annotated training datasets and overfitting problems. However, the loss of function problem in MCFNets remains challenging.

A modified CNN architecture in the non-sampled shearlet transform (NSST) domain was presented in (Hermessi et al., 2018) for medical image fusion feature extraction. The CNN architecture was used to generate feature maps; which were then used to fuse the high-frequency coefficients. The energy attribute function was used to obtain low-frequency coefficients. This method produces more prominent results than the simple NSST methods in terms of multidirectional features and spectral distortions. A CNN with a dual-channel spiking cortical model (DCSCM) was proposed in (Hou et al., 2019) for the MMIF. This method fuses input images using the NSST model followed by a CNN architecture with an adaptive selection rule and DCSCM to obtain high- and low-frequency coefficients. Finally, inverse NSST was applied to obtain a fused image. It is very effective to extract information from dark regions. All these methods overlook the loss of semantic information in a fused image, which leads to boundary blurriness.

An MMIF based on the U-Net method was proposed in (Fan et al., 2019), which resolved the issue of semantic loss. In this method, two U-Net models were merged to construct a new FW-Net model. The encoder (left) and decoder (right) structures of the FW-Nets model follow the structure used in the U-Net model. This model extracts semantic information from an input image using an encoder and reconstructs it using a decoder. Bilinear interpolation functions were used to obtain smooth images. This method achieved prominent results with no semantic conflicts in the fused image. However, it is only applicable to the MRI and CT modalities; other modalities, such as the PET, MR, SPECT, and MR fusion, will be of interest in the future research. A novel method using the generative adversarial network (GAN) was presented in (Nandhini Abirami et al., 2022) for fusing MRI and PET images. The GAN model consisted of two parts: a generator and discriminator. The generator produces the same data distribution as the source image, whereas the discriminator distinguishes the source image from original image. The GAN model is effective in retaining the selected information in the source images. The GAN model overcomes the limitations of data labeling and provides sharp images with less distortion. However, it suffers from convergence and overfitting issues when the generator and discriminator are unbalanced. Fig. 14 shows publication results of MMIF methods in the DL domain. The results were obtained from the Web of Science (WoS).

Table 8
Qualitative results MMIF methods using assessment metrics.

MMIF Method and Publication Year	Domain	the whole brain Atlas (AANLIB)							
		MRI/CT				**MRI/PET**			
		EN	SSIM	SD	MI	EN	SSIM	SD	MI
C. He et al. (He et al., 2010) 2010	Spatial	4.2141	0.9545	60.21	2.4535	3.8541	0.1457	76.21	5.8541
Z. Fu et al. (Fu et al., 2020) 2020	Spatial	4.4522	0.9965	62.35	2.5214	3.8554	0.8547	78.95	5.9981
B.R. Kumar (Kumar, 2014) 2013	Frequency	4.2142	0.8541	59.65	1.5118	3.0284	0.9844	82.54	4.9889
Q. Hu et al. (Hu et al., 2020) 2020	Frequency	5.1101	1.7154	61.84	2.9547	3.6541	0.7498	87.65	5.6542
Sanjay AR et al. (Sanjay et al., 2017) 2017	Fuzzy Set	3.5124	0.5471	63.25	2.5474	4.8541	0.6649	85.65	5.1299
Y. Liu et al. (Liu et al., 2020) 2020	Sparse Rep.	5.2412	1.5424	62.08	3.1204	5.2144	0.5784	92.84	6.3214
F. Fan et al. (Fan et al., 2019) 2019	Deep Learning	6.3214	1.4214	69.54	3.2147	5.0214	0.9241	95.21	6.5521
R. NandhiniAbirami (Nandhini Abirami et al., 2022) 2022	Deep Learning	6.8521	1.2145	75.65	3.5841	6.1524	0.8054	98.54	7.0010
S.D. Ramlal et al. (Ramlal et al., 2019) 2019	Hybrid	6.5841	1.0112	78.95	4.2412	5.2107	0.6671	94.85	7.5211
L. Xu et al. (Xu et al., 2020) 2020	Hybrid	6.8121	1.4329	74.54	3.9842	5.2541	0.5782	97.21	7.1101

5.6. Hybrid domain

As demonstrated by the preceding methods, the MMIF results obtained by single-domain methods are not satisfactory. Consequently, researchers are concentrating on hybrid methods to improve fusion results. In the hybrid method, two or more domain methods are combined, such as the transform and DL domain methods, to improve the final fused image performance (Soundrapandiyan et al., 2017; Singh and Anand, 2019). It also removes noise artifacts and enhances the fused image quality. The DWT and IFS methods described in (Soundrapandiyan et al., 2017) used the DWT method for image decomposition and intuitionistic Fuzzy set rules to fuse the images. This method increases the contrast of a fused image without causing uncertainty. An MMIF method based on PCNN in the NSCT domain was proposed in (Das and Kundu, 2012). In this method, the input images are decomposed using the NSCT method and PCNN, and maximum selection rules are used to combine high- and low-frequency coefficients. Finally, an inverse NSCT is performed to obtain the fused image.

The MMIF method based on the DWT and PCA was proposed in (Sharmila et al., 2013) and achieves better subjective and objective results than the single-domain fusion methods. A combination of swarm intelligence and the PCNN method proposed in (Vickers, 2017) was used to achieve good fusion results. In this method, a prominent technique "And Colony Optimization (ACO)" was implemented for edge detection. The edges are forwarded to the PCNN to produce a fused image. This method outperformed the previous hybrid and conventional methods. In (Ramlal et al., 2019), an improved SWT-NSCT MMIF hybrid method was proposed to achieve superior fusion performance. Here, the NSCT method was implemented to obtain high and low sub-bands of the source images, followed by the SWT method. Entropy squares and improved Laplacians were employed as fusion rules. An inverse NSCT was used to obtain the fused image.

As stated previously, each MMIF fusion method has advantages and disadvantages. However, more efficient algorithms are required to obtain fused images with better visual quality, fewer spectral and spatial distortions, and more detailed information. Table 4 illustrates the MMIF studies in different domains, along with the multimodal modalities combinations, fusion methods, and databases. Table 5 depicts the advantages and limitations of the aforementioned MMIF domains. Fig. 15 shows the results of the MMIF methods in the hybrid domain. The results were obtained from the Web of Science (WoS).

6. Multimodal image fusion combinaton

Each imaging modality has a set of characteristics and limitations, such as MRI imaging, and provides anatomical information but no functional information. MRI does not cause radiation damage to the human body and has a high spatial resolution, which simplifies the clinical process.PET imaging, on the contrary, provides metabolic or functional information in pseudo-color without anatomical information. It has high sensitivity but fails to provide accurate location information in the brain, resulting in spatial distortion. SPECT imaging provides useful information about tumors, but has limited positioning capability. It provides information about blood flow, soft tissues, etc., but has low positioning ability and spatial resolution. X-rays use radiation to produce two-dimensional (2D) images of bones and are typically used to diagnose bone diseases. CT provides more detailed information and is more powerful than X-ray imaging. It is primarily used to diagnose the internal organs of the body in 3D, such as bone fractures, bone tumors, and bone disorders.

Medical image fusion can be accomplished using various techniques, such as the positron emission tomography (PET), PET computed tomography (MRI), CT, and magnetic resonance. These various modality combinations retain their own characteristics, such as the PET/MRI, which is most likely used for the liver, Alzheimer's disease, and tumor detection, whereas the MRI/SPECT image fusion assists in lesion localization. Fig. 16 depicts the trends in studies related to the PET/MRI, MRI/CT, and MRI/SPECT fusion. The results were obtained from the Web of Science (WoS), and the statistical period was 2015–2022.

7. Performance assessment metrics

Subjective/qualitative and objective/quantitative methods were used to assess the quality of the fused images. Qualitative methods include visual inspection of an image, and parameters, such as color, spatial details, and image size, are considered during the

inspection process. However, these methods are time consuming, expensive, and inconvenient (Meher et al., 2019). In objective methods, the fused image is inspected using the statistical parameters. They are further divided into two categories: (1) performance assessment metrics with a reference image and (2) performance assessment metrics without a reference image. Tables 6 and 7 show the commonly used objective method performance assessment metrics with and without the reference images. Each parameter exhibits unique properties.

This review investigates the performance of the MMIF methods for qualitative and quantitative analyses using the commonly used AANLIB medical database. The experiments were carried out with MATLAB 2021a on a Core i74780 CPU with 1.7 GHz and 16 GB RAM. Figs. 17 and 18 show the qualitative results of the MRI/CT and MRI/PET using the various MMIF methods, such as (NSCT (Kumar, 2014) S_Link 1), (NSST-PAPCNN (Singh et al., 2015) S_Link 2), (IFCNN (Zhang et al., 2020) S_Link 3), and (N-Fuzzy (Das and Kundu, 2015) S_Link 4). The source code for these MMIF methods is provided in the Supporting Materials. The datasets may be requested from the corresponding authors.

Fig. 17 (a) and (b) show the MRI and CT images. Fig. 17 (c) shows that some complementary information is not visible, Fig. 17 (d) shows some blurring effects, and Fig. 17 (e) and (f) are visually better.

Fig. 18 (a) and (b) show the MRI and PET images, respectively; Fig. 18 (c) shows that the fused image is severely degraded and has a low contrast; Fig. 18 (d) shows that the fused image has spatial distortion; Fig. 18 (e) is visually better; and Fig. 18 (f) shows that the fused image is less enhanced. According to our findings, IFCNN (Zhang et al., 2020) and N-Fuzzy (Das and Kundu, 2015) have satisfactory qualitative results. Considering both decomposition level and time complexity, IFCNN (Zhang et al., 2020) and N-Fuzzy (Das and Kundu, 2015) performs better than others. Another important factor that affects the quality of fused images is the design of fusion rules for high- and low-frequency sub-bands of source images. Image fusion rules play an important role in getting complementary information from input images. In our estimation (visual analysis and later on verified using statistical metrics), color changes are important visual information for the fusion of PET and MR images. To preserve anatomical structures while better keeping color changes in the fused image, high-frequency sub-bands from both the MR image and I-component of PET image should be considered. Therefore, in the fusion method, each high-frequency subband coefficient from the same location of MR image and I-component of PET image is selected by specific fusion rule. The larger transform values in these bands correspond to sharper brightness changes and thus to the salient features in the image such as edges, lines, and region boundaries are highlighted.

In this review, MMIF methods from the various fusion domains were collected and their outcomes were compared using assessment metrics (EN, SSIM, SD, and MI). The performance evaluation metrics used in this research work are Standard Deviation (SD) *to* compute the intensity variation of the fused image, Entropy (E) to compute the amount of information in the fused image, Structure Similarity Index Measure (SSIM) to compute the similarities between original and fused image. Table 8 presents the quantitative assessment results.

Table 8 shows that the DL methods performed better for MRI/CT integration, whereas the hybrid methods performed well for MRI/PET integration, which means the fused image has high resolution. Similarly, frequency domain methods outclass the other methods in term of similarity information (SSIM Values). Lastly, hybrid methods achieved good results in term of SD and MI, which means that detailed information is transferred to the fused image and the fused image has all the complementary details. From quantitative and qualitative results, it is concluded that each method/technique has its own drawbacks and advantages such as spatial domain methods are simple and faster to compute. However, these methods have been unsuccessful in real-world scenarios. The application of new methods to MMIF remains a great challenge in this filed.

8. Shortcomings and future directions

This review covers almost all the recent and widely used MMIF methods. Spatial domain methods are simpler, faster to compute, and provide better color visualization. However, these methods have been unsuccessful in real-world scenarios. The fused image exhibited spectral distortion and sharpening issues. The frequency-domain methods overcome the issue of spectral distortion and achieve high SSIM values with good edge information. However, the final fused image using the frequency domain has less spatial detail, and activity-level measurements are difficult (Huang et al., 2020; Masood et al., 2017; Sharma et al., 2020). The Fuzzy and SR domain methods performed well, and the fused images exhibited less spectral distortion, better visual quality, and extracted detailed features. However, these methods involve image registration, optimization, and overfitting issues (Li and Yin, 2011; Bavirisetti et al., 2017; Bhat and Koundal, 2021). Deep learning methods achieve an optimized fused image and high-intensity variation (EN), as shown in Table 8. DL methods are also effective in extracting information from dark regions. However, these methods suffer from semantic loss, convergence, and overfitting. The Hybrid domain methods performed well in terms of (SD) and (MI). In other words, the fused image contains all the complementary information and has smooth edges. However, these methods suffer from nonuniformity and require a long time to train large datasets (Atrey et al., 2010).

Researchers have presented several MMIF methods; however, each method has its own drawbacks. Moreover, the majority of MMIF methods are based on core methods, and existing problems, such as spectral distortion, overfitting, and feature extraction, have been improved but not completely solved. The application of novel algorithms to MMIF remains a significant challenge in this field. Considering the aforementioned issues, the following are potential areas for future research:

i. Challenges in decomposing coefficients using multi-scale decomposition methods for MMIF.
ii. Challenges in fusing multimodal images without background noise.
iii. Developing DL algorithms to reduce long data training times, overfitting, and convergence problems.
iv. Challenges in improving region of interest in source images before fusion process
v. Challenges in creating a free online dataset for different organs (liver, spleen, and bone marrow) to evaluate MMIF methods. According to Fig. 4, only the AANLIB database dominates the remaining fields.

This review article covered almost all areas of MMIF process such as (i) medical imaging modalities, (ii) multimodal medical image databases, (iii) MMIF steps/rules, (iv) MMIF methods, (v) modalities integration, (vi) performance evaluation and empirical results, (vii) current modalities strengths and limitations, and (viii) future directions. However, this review still required more discussion on various medical imaging datasets (categorization), application areas, and imaging modalities with respect to their weaknesses and strengths.

9. Conclusion

The basic objective of MMIF is to enhance the fused image. The MMIF field was thoroughly discussed in this review, which began

by providing a thorough description of different medical imaging modalities, sources of generation, and invasive and non-invasive methods. Subsequently, comparisons of publicly available online multimodal medical databases and their use in research over the last five years were discussed in detail. Next, a brief explanation of the MMIF steps was provided. MMIF methods, including spatial, frequency, Fuzzy set, sparse representation, DL, and hybrid domains, were discussed in detail. Subsequently, an overview of multimodal modalities integration was presented. Objective and subjective image quality assessment metrics were thoroughly discussed. Subsequently, the various MMIF methods were evaluated using these quality-assessment metrics. Finally, the limitations of MMIF methods and future directions were discussed. In this review, it was observed that the fusion results of the DL and Hybrid domain methods outperformed those of other fusion methods. Nevertheless, owing to the numerous issues discussed earlier, it is challenging to determine, which MMIF method is best suited for the types of integrated modalities. Such issues can be addressed by expanding our knowledge of MMIF methods to assist in clinical diagnosis.

Supporting materials

[S_Link 1] https://github.com/zhiqinzhu123/Source-code-of-medical-image-fusion-in-NSCT-domain
[S_Link 2] https://github.com/yuliu316316/NSST-PAPCNN-Fusion
[S_Link 3] https://github.com/uzeful/IFCNN
[S_Link 4] https://github.com/HarrisXia/image-fusion-zoo

Declaration of competing interest

The authors declare that they have no known competing financial interests or personal relationships that could have appeared to influence the work reported in this paper.

Acknowledgements

This work was supported in part by the National Research Foundation of Korea (NRF) grant 2022R1G1A1003531, 2022R1A4A3018824, RS-2023-00230593 and Institute of Information and Communications Technology Planning and Evaluation (IITP) grant IITP-2023-2020-0-01741, RS-2022-00155885 funded by the Korea government (MSIT).

References

AANLIB. http://www.med.harvard.edu/AANLIB/home.html (Accessed 5 January 2020).
ADNI, 2022. https://adni.loni.usc.edu/ (Accessed 10 November 2022).
Andreu-Perez, J., Poon, C.C., Merrifield, R.D., Wong, S.T., Yang, G.Z., 2015. Big data for health. IEEE J. Biomed. Health Inform. 19 (4), 1193–1208.
Arif, M., Wang, G., 2020. Fast curvelet transform through genetic algorithm for multimodal medical image fusion. Soft. Comput. 24 (3), 1815–1836.
Atanassov, K.T., 1994. New operations defined over the intuitionistic fuzzy sets. Fuzzy Set. Syst. 61 (2), 137–142.
Atrey, P.K., Hossain, M.A., El Saddik, A., Kankanhalli, M.S., 2010. Multimodal fusion for multimedia analysis: a survey. Multimedia Syst. 16 (6), 345–379.
Azam, M.A., Khan, K.B., Aqeel, M., Chishti, A.R., Abbasi, M.N., 2020. Analysis of the MIDAS and OASIS biomedical databases for the application of multimodal image processing. In: Intelligent Technologies and. Applications (INTAP 2019) 2020, 581–592.
Aysha, S., Tirupal, T., sha. Image fusion of medical images based on Fuzzy set. Elixir Digital Processing 96, 41225–41228.
Azam, M.A., Khan, K.B., Ahmad, M., Mazzara, M., 2021. Multimodal medical image registration and fusion for quality Enhancement. Cmc-Comput. Mater. Contin 68, 821–840.
Balasubramaniam, P., Ananthi, V.P., 2014. Image fusion using intuitionistic fuzzy sets. Information Fusion 20, 21–30.
Bashir, R., Junejo, R., Qadri, N.N., Fleury, M., Qadri, M.Y., 2019. SWT and PCA image fusion methods for multi-modal imagery. Multimed. Tools Appl. 78 (2), 1235–1263.
Bavirisetti, D.P., Kollu, V., Gang, X., Dhuli, R., 2017. Fusion of MRI and CT images using guided image filter and image statistics. Int. J. Imaging Syst. Technol. 27 (3), 227–237.
Bhat, S., Koundal, D., 2021. Multi-focus image fusion techniques: a survey. Artif. Intell. Rev. 54 (8), 5735–5787.
Bhatnagar, G., Wu, Q.J., Liu, Z., 2015. A new contrast based multimodal medical image fusion framework. Neurocomputing 157, 143–152.
Bhosale, Y.H., Patnaik, K.S., 2023. Bio-medical imaging (X-ray, CT, ultrasound, ECG), genome sequences applications of deep neural network and machine learning in diagnosis, detection, classification, and segmentation of COVID-19: a Meta-analysis & systematic review. Multimed. Tools Appl., 1–54
Biswas, B., Sen, B.K., 2019. Color PET-MRI medical image fusion combining matching regional spectrum in shearlet domain. International Journal of Image and Graphics 19 (01), 1950004.
Daneshvar, S., Ghassemian, H., 2010. MRI and PET image fusion by combining IHS and retina-inspired models. Information fusion 11 (2), 114–123.
Das, S., Kundu, M.K., 2012. NSCT-based multimodal medical image fusion using pulse-coupled neural network and modified spatial frequency. Med. Biol. Eng. Compu. 50 (10), 1105–1114.
Das, S., Kundu, M.K., 2013. A neuro-fuzzy approach for medical image fusion. IEEE Trans. Biomed. Eng. 60 (12), 3347–3353.
Das, S., Kundu, M.K., 2015. Corrections to "A Neuro-Fuzzy Approach for Medical Image Fusion" [Dec 13 3347–3353]. IEEE Trans. Biomed. Eng. 62 (4), 1226.
Dolly, J.M., Nisa, A.K., 2019. A survey on different multimodal medical image fusion techniques and methods. In: International Conference on Innovations in Information and Communication Technology (ICIICT 2019), 1–5.
Du, J., Li, W., Lu, K., Xiao, B., 2016. An overview of multi-modal medical image fusion. Neurocomputing 215, 3–20.
Du, J., Li, W., Xiao, B., Nawaz, Q., 2016. Union Laplacian pyramid with multiple features for medical image fusion. Neurocomputing 194, 326–339.
El-Gamal, F., Elmogy, M., Atwan, A., 2016. Current trends in medical image registration and fusion. Egypt. Inform. J. 17 (1), 99–124.
El-Gamal, F.E.Z.A., Elmogy, M., Atwan, A., 2016. Current trends in medical image registration and fusion. Egyptian Informatics Journal 17 (1), 99–124.
El-Hoseny, H.M., Abd El-Rahman, W., El-Rabaie, E.S.M., Abd El-Samie, F.E., Faragallah, O.S., 2018. An efficient DT-CWT medical image fusion system based on modified central force optimization and histogram matching. Infrared Phys. Technol. 94, 223–231.
Fan, F., Huang, Y., Wang, L., Xiong, X., Jiang, Z., Zhang, Z., Zhan, J., 2019. A semantic-based medical image fusion approach. arXiv preprint arXiv:1906.00225.
Faragallah, O.S., El-Hoseny, H., El-Shafai, W., Abd El-Rahman, W., El-Sayed, H.S., El-Rabaie, E.S.M., Geweid, G.G., 2020. A comprehensive survey analysis for present solutions of medical image fusion and future directions. IEEE Access 9, 11358–11371.
Fu, Z., Zhao, Y., Xu, Y., Xu, L., Xu, J., 2020. Gradient structural similarity based gradient filtering for multi-modal image fusion. Information Fusion 53, 251–268.
Gomathi, P.S., Kalaavathi, B., 2014. Medical Image Fusion Based On Redundant Wavelet Transform and Morphological Processing. International Journal of Computer and Information Engineering 8 (6), 1018–1022.
Goyal, B., Dogra, A., Lepcha, D.C., Koundal, D., Alhudhaif, A., Alenezi, F., Althubiti, S. A., 2022. Multi-modality image fusion for medical assistive technology management based on hybrid domain filtering. Expert Syst. Appl. 209, 118283.
Haddadpour, M., Daneshvar, S., Seyedarabi, H., 2017. PET and MRI image fusion based on combination of 2-D Hilbert transform and IHS method. Biomedical journal 40 (4), 219–225.
Haidekker, M.A., 2013. X-Ray Projection Imaging. In: Medical Imaging Technology. SpringerBriefs in Physics, pp. 13–35.
Haribabu, M., Guruviah, V., Yogarajah, P., 2023. Recent Advancements in Multimodal Medical Image Fusion Techniques for Better Diagnosis: An overview. Current Medical Imaging 19 (7), 673–694.
He, C., Liu, Q., Li, H., Wang, H., 2010. Multimodal medical image fusion based on IHS and PCA. Procedia Eng. 7, 280–285.
Heba, M., Rabaieb, E.S.M.E., Elrahmana, W.A., Faragallahc, O.S., El-Samieb, F.E.A., 2017. Medical image fusion: A literature review present solutions and future directions. Minufiya J. of Electronic Engineering Research (MJEER) 26 (2).
Hermessi, H., Mourali, O., Zagrouba, E., 2018. Convolutional neural network-based multimodal image fusion via similarity learning in the shearlet domain. Neural Comput. & Applic. 30 (7), 2029–2045.
Hermessi, H., Mourali, O., Zagrouba, E., 2021. Multimodal medical image fusion review: Theoretical background and recent advances. Signal Process. 183, 108036.
Hou, R., Zhou, D., Nie, R., Liu, D., Ruan, X., 2019. Brain CT and MRI medical image fusion using convolutional neural networks and a dual-channel spiking cortical model. Med. Biol. Eng. Compu. 57 (4), 887–900.
Hu, Q., Hu, S., Zhang, F., 2020. Multi-modality medical image fusion based on separable dictionary learning and Gabor filtering. Signal Process. Image Commun. 83, 115758.

Huang, B., Yang, F., Yin, M., Mo, X., Zhong, C., 2020. A review of multimodal medical image fusion techniques. Computational and mathematical methods in medicine.
Ismail, W.Z.W., Sim, K.S., 2011. Contrast enhancement dynamic histogram equalization for medical image processing application. Int. J. Imaging Syst. Technol. 21 (3), 280–289.
James, A.P., Dasarathy, B.V., 2014. Medical image fusion: A survey of the state of the art. Information fusion 19, 4–19.
Jian, L., Yang, X., Zhou, Z., Zhou, K., Liu, K., 2018. Multi-scale image fusion through rolling guidance filter. Futur. Gener. Comput. Syst. 83, 310–325.
Kaur, H., Koundal, D., Kadyan, V., 2021. Image fusion techniques: a survey. Arch. Comput. Meth. Eng. 28 (7), 4425–4447.
Khan, S.U., Wang, Y.C., Chai, S.S., 2013. A novel noise removal technique of X-ray carry-on luggage for detection of contraband/illicit object (s). International Journal of Engineering and Advance Technology 2 (3), 94–99.
Krishnamoorthy, S., Soman, K.P., 2010. Implementation and comparative study of image fusion algorithms. International Journal of Computer Applications 9 (2), 25–35.
Krizhevsky, A., Sutskever, I., Hinton, G.E., 2017. Imagenet classification with deep convolutional neural networks. Commun. ACM 60 (6), 84–90.
Kumar, S.V., 2014. Directive contrast based multimodal medical image fusion in NSCT with DWT domain. Int. Journal of Engineering Trends Technology 9 (6), 288–294.
Li, S., Yin, H., 2011. Multimodal image fusion with joint sparsity model. Opt. Eng. 50, (6) 067007.
Liang, X., Hu, P., Zhang, L., Sun, J., Yin, G., 2019. MCFNet: Multi-layer concatenation fusion network for medical images fusion. IEEE Sens. J. 19 (16), 7107–7119.
Liu, Y., Chen, X., Peng, H., Wang, Z., 2017. Multi-focus image fusion with a deep convolutional neural network. Information Fusion 36, 191–207.
Liu, D., Chen, X., Peng, D., 2018. Cosine similarity measure between hybrid intuitionistic fuzzy sets and its application in medical diagnosis. Comput. Math. Methods Med.
Liu, D., Chen, X., Peng, D., 2018. The intuitionistic fuzzy linguistic cosine similarity measure and its application in pattern recognition. Complexity.
Liu, Y., Yang, X., Zhang, R., Albertini, M.K., Celik, T., Jeon, G., 2020. Entropy-based image fusion with joint sparse representation and rolling guidance filter. Entropy 22 (1), 118.
Maini, R., Aggarwal, H., 2010. A comprehensive review of image enhancement techniques. arXiv preprint arXiv:1003.4053.
Maqsood, S., Javed, U., 2020. Multi-modal medical image fusion based on two-scale image decomposition and sparse representation. Biomed. Signal Process. Control 57, 101810.
Masood, S., Sharif, M., Yasmin, M., Shahid, M.A., Rehman, A., 2017. Image fusion methods: a survey. J. Eng. Sci. Technol. Rev. 10 (6).
Meher, B., Agrawal, S., Panda, R., Abraham, A., 2019. A survey on region based image fusion methods. Information Fusion 48, 119–132.
Memon, F., Unar, M.A., Memon, S., 2015. Image quality assessment for performance evaluation of focus measure operators. Mehran Univ. Res. J. Eng. Technol. 34 (4), 379–386.
Mhangara, P., Mapurisa, W., Mudau, N., 2020. Comparison of image fusion techniques using satellite pour l'Observation de la Terre (SPOT) 6 satellite imagery. Appl. Sci. 10 (5), 1881.
Mishra, D., Palkar, B., 2015. Image fusion techniques: a review. International Journal of Computer Applications 130 (9), 7–13.
MITA. https://www.medicalimaging.org/about-mita/medical-imaging-primer/ (Accessed 10 November 2022).
Nandhini Abirami, R., Durai Raj Vincent, P.M., Srinivasan, K., Manic, K.S., Chang, C.Y., 2022. Multimodal medical image fusion of positron emission tomography and magnetic resonance imaging using generative adversarial networks. Behav. Neurol.
Narsaiah, M.N., Vathsal, S., Reddy, D.V., 2018. A Survey on Image Fusion Requirements, Techniques, Evaluation Metrics, and Its Applications. International Journal of. Eng. Technol. 7 (2.20), 260–266.
O'Mahony, D., Gandjbakhche, A.H., Hassan, M., Vogel, A., Yarchoan, R., 2008. Imaging techniques for Kaposi Sarcoma (KS). J. HIV Ther. 13 (3), 65.
Parmar, K., Kher, R., 2012. A comparative analysis of multimodality medical image fusion methods. In: Asia Modelling Symposium (AMS 2012), 93–97.
Polinati, S., Dhuli, R., 2020. Multimodal medical image fusion using empirical wavelet decomposition and local energy maxima. Optik 205, 163947.
Princess, M.R., Kumar, V.S., Begum, M.R., 2014. Comprehensive and comparative study of different image fusion techniques. Int. J. Adv. Res. Electr. Electron. Instrum. Eng, 11800–11806.
Rajalingam, B., Priya, R., 2018. Review of multimodality medical image fusion using combined transform techniques for clinical application. International Journal of Scientific Research in Computer Science Applications and Management Studies 7 (3), 1–8.
Ramlal, S.D., Sachdeva, J., Ahuja, C.K., Khandelwal, N., 2018. Multimodal medical image fusion using non-subsampled shearlet transform and pulse coupled neural network incorporated with morphological gradient. SIViP 12 (8), 1479–1487.
Ramlal, S.D., Sachdeva, J., Ahuja, C.K., Khandelwal, N., 2019. An improved multimodal medical image fusion scheme based on hybrid combination of nonsubsampled contourlet transform and stationary wavelet transform. Int. J. Imaging Syst. Technol. 29 (2), 146–160.
Reena Benjamin, J., Jayasree, T., 2018. Improved medical image fusion based on cascaded PCA and shift invariant wavelet transforms. Int. J. Comput. Assist. Radiol. Surg. 13 (2), 229–240.
Sadjadi, F., 2005. Comparative image fusion analysais. CVPR workshop. 8–8.
Sanjay, A.R., Soundrapandiyan, R., Karuppiah, M., Ganapathy, R., 2017. CT and MRI image fusion based on discrete wavelet transform and Type-2 fuzzy logic. International Journal of Intelligent Engineering and Systems 10 (3), 355–362.
Sebastian, J., King, G.G., 2021. Fusion of multimodality medical images-A review. In: Smart Technologies, Communication and Robotics (STCR 2021), pp. 1–6.
Sharma, A.M., Dogra, A., Goyal, B., Vig, R., Agrawal, S., 2020. From pyramids to state-of-the-art: a study and comprehensive comparison of visible–infrared image fusion techniques. IET Image Proc. 14 (9), 1671–1689.
Sharmila, K., Rajkumar, S., Vijayarajan, V. 2013. Hybrid method for multimodality medical image fusion using discrete wavelet transform and entropy concepts with quantitative analysis. In: *International Conference on Communication and Signal Processing (ICCSP 2013)*, 489-493.
Shreyamsha Kumar, 2015. Image fusion based on pixel significance using cross bilateral filter. Signal, image and video processing 9, 1193–1204.
Singh, S., Anand, R.S., 2019. Multimodal medical image fusion using hybrid layer decomposition with CNN-based feature mapping and structural clustering. IEEE Trans. Instrum. Meas. 69 (6), 3855–3865.
Singh, B., Gautam, R., Kumar, S., Kumar, B.V., Nongthomba, U., Nandi, D., Umapathy, S., 2012. Application of vibrational microspectroscopy to biology and medicine. CURRENT SCIENCE 102 (2), 232.
Singh, S., Gupta, D., Anand, R.S., Kumar, V., 2015. Nonsubsampled shearlet based CT and MR medical image fusion using biologically inspired spiking neural network. Biomed. Signal Process. Control 18, 91–101.
Singh, R., Khare, A., 2014. Fusion of multimodal medical images using Daubechies complex wavelet transform–A multiresolution approach. Information fusion 19, 49–60.
Sivasangumani, S., Gomathi, P.S., Kalaavathi, B., 2015. Regional firing characteristic of PCNN-based multimodal medical image fusion in NSCT domain. Int. J. Biomed. Eng. Technol. 18 (3), 199–209.
Soundrapandiyan, R., Karuppiah, M., Kumari, S., Kumar Tyagi, S., Wu, F., Jung, K.H., 2017. An efficient DWT and intuitionistic fuzzy based multimodality medical image fusion. Int. J. Imaging Syst. Technol. 27 (2), 118–132.
Stokking, R., Zuiderveld, K.J., Viergever, M.A., 2001. Integrated volume visualization of functional image data and anatomical surfaces using normal fusion. Hum. Brain Mapp. 12 (4), 203–218.
Subramanian, P., Alamelu, N.R., Aramudhan, M., 2015. Fusion of multispectral and panchromatic images and its quality assessment. J. Eng. Appl. Sci. 10 (9), 2–24.
TCIA, 2022. https://www.cancerimagingarchive.net/ (Accessed 5 November 2022).
Teng, J., Wang, S., Zhang, J., Wang, X., 2010. Neuro-fuzzy logic based fusion algorithm of medical images. In: international Congress on Image and Signal Processing. 4, 1552–1556.
Tirupal, T., Mohan, B.C., Kumar, S.S., 2017. Multimodal medical image fusion based on Sugeno's intuitionistic fuzzy sets. ETRI J. 39 (2), 173–180.
Tirupal, T., Chandra Mohan, B., Srinivas Kumar, S., 2019. Multimodal medical image fusion based on yager's intuitionistic fuzzy sets. Iranian Journal of Fuzzy Systems 16 (1), 33–48.
Tirupal, T., Chandra Mohan, B., Srinivas Kumar, S., 2021. "Multimodal medical image fusion techniques–a review." Current Signal Transduction. Therapy 16 (2), 142–163.
Torrado-Carvajal, A., Herraiz, J.L., Hernandez-Tamames, J.A., San Jose-Estepar, R., Eryaman, Y., Rozenholc, Y., Malpica, N., 2016. Multi-atlas and label fusion approach for patient-specific MRI based skull estimation. Magn. Reson. Med. 75 (4), 1797–1807.
Vickers, N.J., 2017. Animal communication: when i'm calling you, will you answer too? Curr. Biol. 27 (14), R713–R715.
Wang, H.H., 2004. A new multiwavelet-based approach to image fusion. J. Math. Imaging Vision 21 (2), 177–192.
Wang, W., Chang, F., 2011. A Multi-focus Image Fusion Method Based on Laplacian Pyramid. J. Comput. 6 (12), 2559–2566.
Victor, I.M., Victor, V.M., 2014. Medical Imaging Technology.
Wang, Y.P., Dang, J.W., Li, Q., & Li, S., 2007. Multimodal medical image fusion using fuzzy radial basis function neural networks. In: 2007 International Conference on Wavelet Analysis and Pattern Recognition. IEEE, vol. 2, pp. 778–782.
Wang, Z., Ma, Y., 2008. Medical image fusion using m-PCNN. Information Fusion 9 (2), 176–185.
Xiaoxue, X., Fucheng, C., Weiwei, S., Fu, L., 2015. Multi-modal Medical Image Fusion Based on Non-subsampled Shearlet Transform. International Journal of Signal Processing, Image Processing and Pattern Recognition 8 (2), 41–48.
Xu, L., Si, Y., Jiang, S., Sun, Y., Ebrahimian, H., 2020. Medical image fusion using a modified shark smell optimization algorithm and hybrid wavelet-homomorphic filter. Biomed. Signal Process. Control 59, 101885.
https://github.com/QIICR/dcmqi, https://github.com/herrmannlab/highdicom
Yang, L., Guo, B.L., Ni, W., 2008. Multimodality medical image fusion based on multiscale geometric analysis of contourlet transform. Neurocomputing 72 (1–3), 203–211.
Yang, G., Li, M., Chen, L., Yu, J., 2015. The nonsubsampled contourlet transform based statistical medical image fusion using generalized Gaussian density. Comput. Math. Methods Med.
Yang, Y., Park, D.S., Huang, S., Rao, N., 2010. Medical image fusion via an effective wavelet-based approach. EURASIP journal on advances in signal processing 2010, 1–13.

Yang, Y., Tong, S., Huang, S., Lin, P., 2014. Dual-tree complex wavelet transform and image block residual-based multi-focus image fusion in visual sensor networks. Sensors 14 (12), 22408–22430.
Yang, Y., Que, Y., Huang, S., Lin, P., 2016. Multimodal sensor medical image fusion based on type-2 fuzzy logic in NSCT domain. IEEE Sens. J. 16 (10), 3735–3745.
Yin, M., Liu, X., Liu, Y., Chen, X., 2018. Medical image fusion with parameter-adaptive pulse coupled neural network in nonsubsampled shearlet transform domain. IEEE Trans. Instrum. Meas. 68 (1), 49–64.
Zarif, S., Faye, I., Rohaya, D., 2014. A comparative study of different image completion techniques. In: International Conference on Computer and Information Sciences (ICCOINS 2014), pp. 1–6.
Zhang, Y., Liu, Y., Sun, P., Yan, H., Zhao, X., Zhang, L., 2020. IFCNN: A general image fusion framework based on convolutional neural network. Information Fusion 54, 99–118.
Zhang, L., Lu, H., Serikawa, S., 2012. Maximum local energy method for multispectral image fusion in remote sensing system. Disaster advances 5 (4), 17–20.
Zhou, T., Ruan, S., Canu, S., 2019. A review: Deep learning for medical image segmentation using multi-modality fusion. Array 3, 100004.